Clarkson University defy convention

Integrated Surface-Subsurface Modeling

Weiming Wu, PhD
Professor
Dept. of Civil and Environmental Eng.
Clarkson University
Potsdam, NY 13699, USA

Updated on Oct. 9, 2014

Coupled 2-D Surface and 3-D Subsurface Model for Flow, Soil Erosion, and Contaminant Transport

Zhiguo He’s Dissertation Topic (2007)

Supervised by Weiming Wu

Content

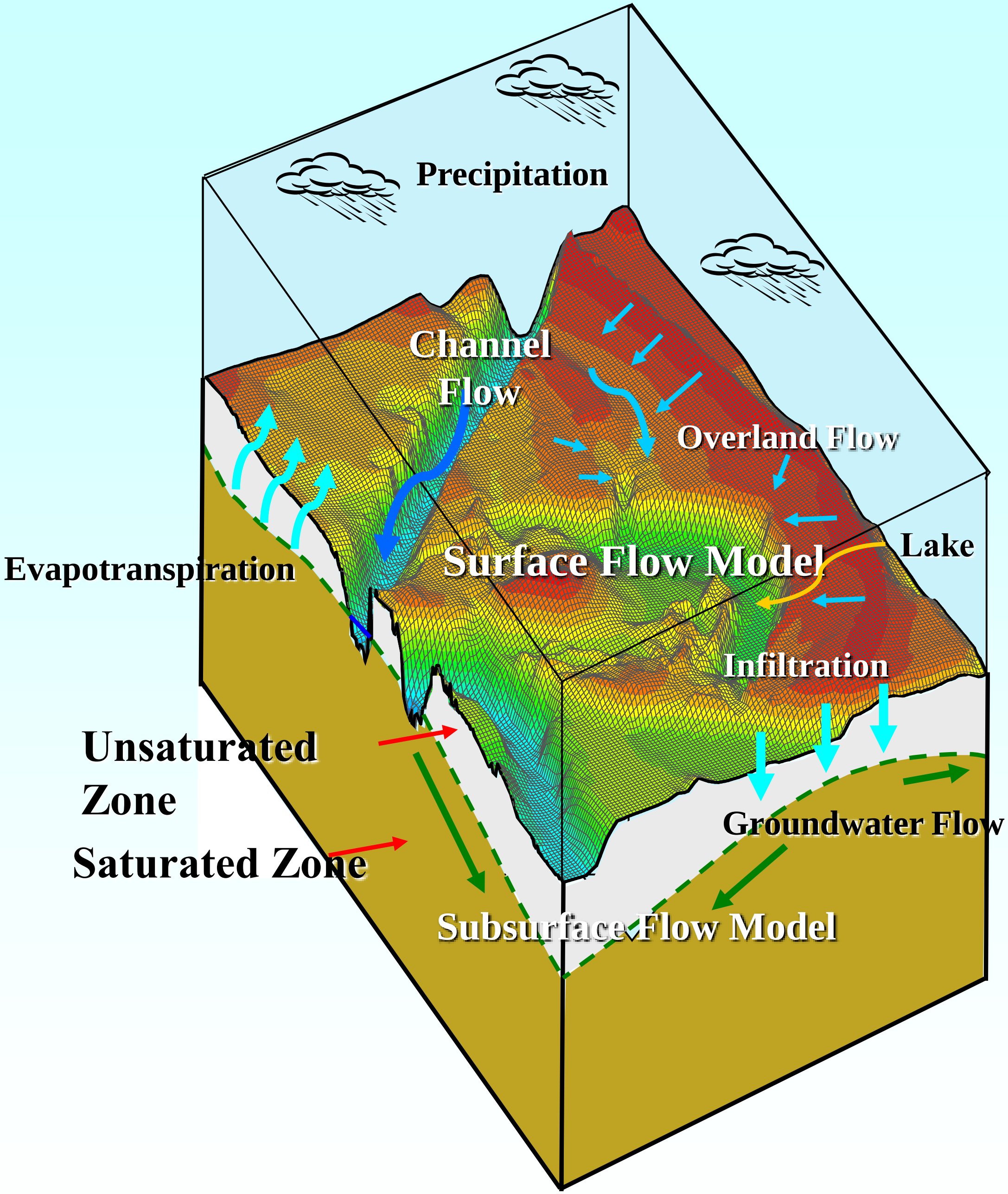

Or more:
snowmelt, recharge, upland soil erosion, contaminant transport, etc.

These hydrological processes involve both surface and subsurface domains that often behave in a coupled manner.

Research (*Wallach et al., 1997*) has pointed out that neglecting the interaction between surface and subsurface can cause errors in surface runoff prediction. Coupled model provides more accurate predictions.

Physically-based watershed models coupling surface and subsurface are widely believed to provide greater opportunities to evaluate hydrologic response of rainfall-runoff, infiltration, and groundwater discharge (e.g. *Morita and Yen, 2002; Kollet and Maxwell, 2006*).

They also have immense ability to forecast the movement of pollutants and sediment (*Beven, 1985; Heppner et al., 2006*).

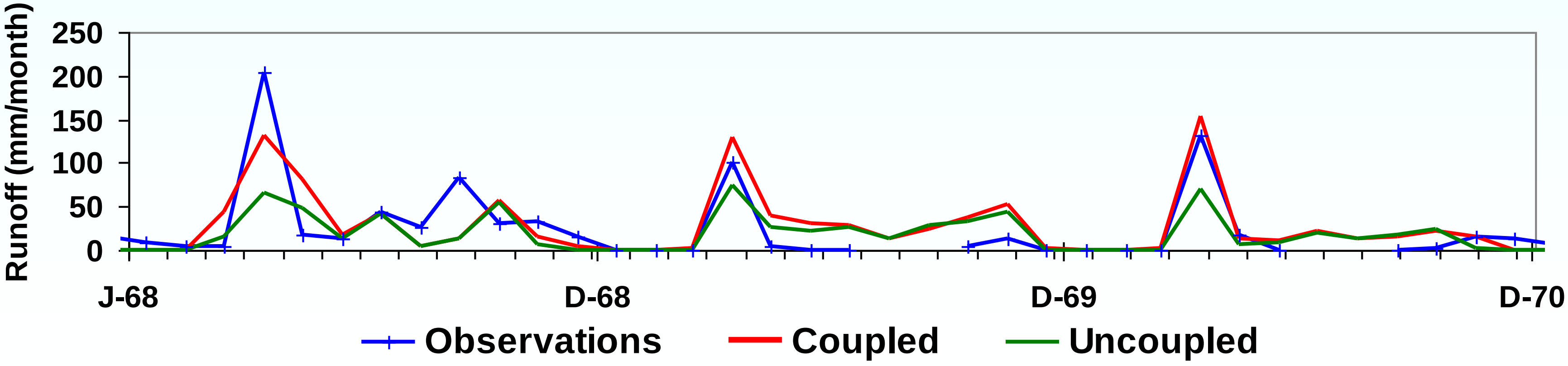

Physically-Based Integrated Hydrological Modeling

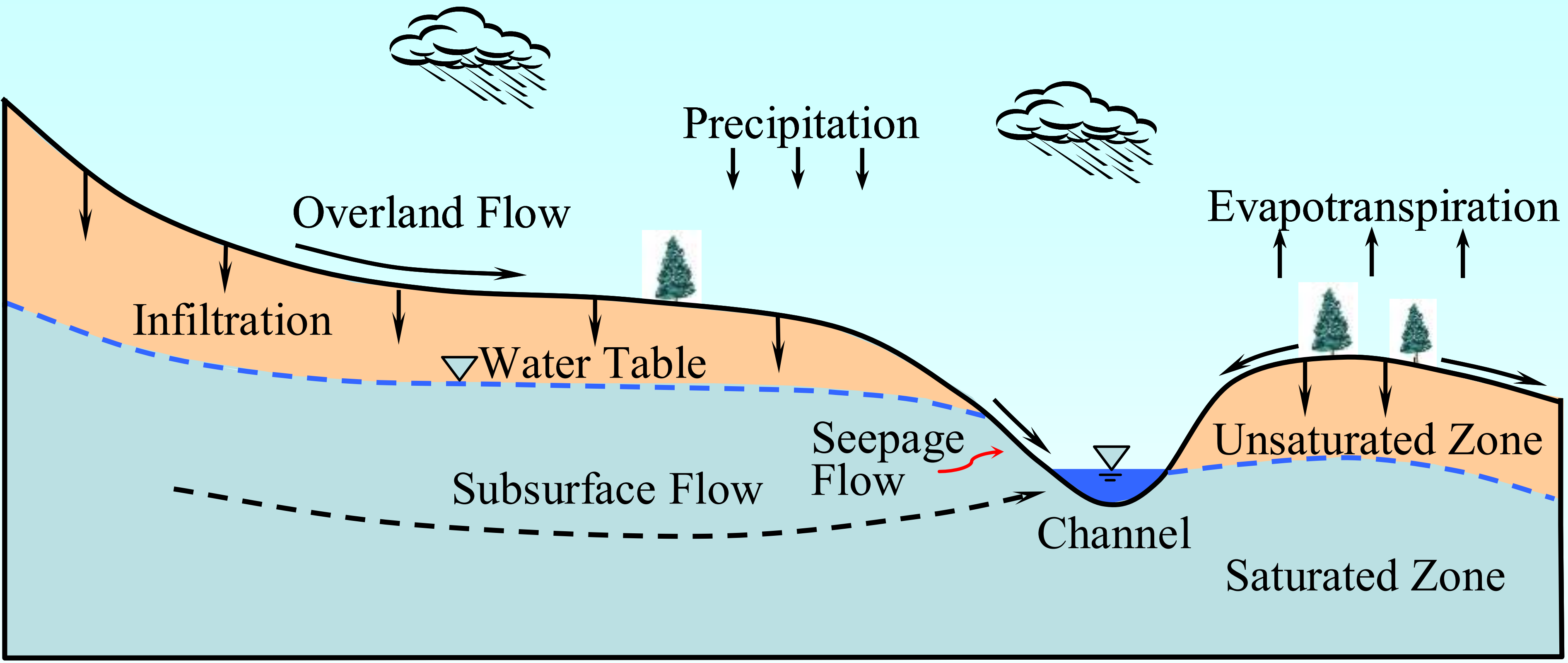

Three components:

- **Surface flow PDE:** **(a) Full Saint-Venant equations, (b) Quasi-steady dynamic wave (c) Kinematic wave, (d) Diffusion wave approximation**
- **Subsurface flow PDE:** **Variably saturated Richards equation: pressure-head form, moisture-base form, mixed form**
- **Interaction:** **Common internal boundary conditions of infiltration and pressure head at the interface.**

Brief Overview on Integrated Watershed Models

Blueprint Freeze and Harlan (1969)

Early stage Simple 1-D externally coupled models
(e.g. *Smith and Woolhiser, 1971;*
Akan and Yen, 1981)

Now Fully coupled models — 2-D surface/3-D subsurface
(e.g. *VanderKwaak and Loague, 2001;*
Morita and Yen, 2002;
Panday and Huyakorn, 2004;
Kollet and Maxwell, 2006;
MIKE SHE, 1995; TRUST, 1995;
InHM, 1999; MODHMS, 2004;
RSM, 2005)

Reference	Surface flow			Subsurface flow	
	Channel	Overland	Solution Method	Equation	Solution Method
Pinder and Sauer (1971)	1D, SV	n/a	Staggered explicit scheme	2D, S	ADI
Smith and Woolhiser (1971)	n/a	1D, KW	Lax-Wendroff, explicit	1D, U	Crank-Nicholson
Freeze (1972)	1D, SV	n/a	Single step Lax-Wendroff	3D, U/S	SLOR
Akan and Yen (1981)	n/a	1D, SV	4-point implicit	2D, U/S	SLOR
Schmitz et al. (1985)	n/a	1D, SV	Implicit method of Characteristics	1D, Parlange	Algebraic FEM
Liggett and Dillon (1985)	1D, KW	n/a	Muskingum-Cunge	1D, U	BIEM
SHE (Abbott et al., 1982&1986)	n/a	2D, DW	Abbott 6-point Implicit	1D, U	Full implicit
Di Giammarco et al. (1994)	1D	2D, DW	Finite element, Crank-Nicholson	1D, U; 2D, S	Finite element
SHE (Bathurst et al., 1996)	1D, SV	2D, DW	Modified Gauss-Seidel	1D, U; 2D, S	Implicit, SOR
Wallach et al. (1997)	n/a	1D, KW	Implicit, Newton iteration	1D, U/S	Implicit
Bradford and Katopodes (1998)	2D, Re	2D, Re	Marker-and-cell, moving grid	2D, U	Gelarkin FEM
Singh and Bhallamudi (1998)	n/a	1D, SV	ENO scheme, Explicit	2D, U	Crank-Nicholson
InHM (VanderKwaak, 1999)	2D, DW	2D, DW	Implicit, Control volume FEM	3D, U/S	Implicit, CVFEM
Morita and Yen (2002)	2D, DW	2D, DW	Saul'yev's downstream scheme	3D, U/S	Larkin's ADE
Panday and Kuyakorn (2004)	1D, DW	2D, DW	Implicit, Newton-Raphson	3D, U/S	Implicit, Newton-Raphson
RSM (Wasantha Lal et al., 2005)	1D, DW	2D, DW	Implicit FVM	2D, S	Implicit FVM
Kollet and Maxwell (2006)	2D, KW	2D, KW	Implicit, Newton-Krylov	3D, U/S	Implicit, Newton-Krylov

Conductance Concept

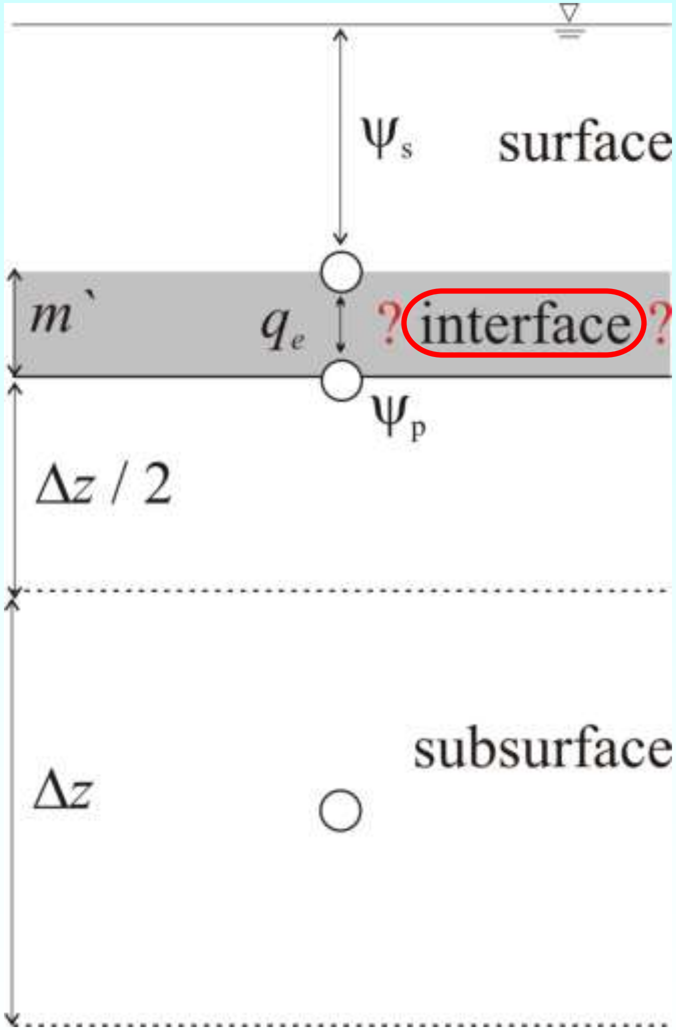

$$\frac{\partial \psi_s}{\partial t} = \nabla \vec{v}\,\psi_s - q_r(x) - q_e(x)$$

$$q_e(x) = \lambda(x)(\psi_s - \psi_p)$$

Proportionality constant

Water head gradient

$$S_s S_w \frac{\partial \psi_p}{\partial t} + \phi \frac{\partial S_w(\psi_p)}{\partial t} = \nabla \cdot q + q_s$$

However, recent studies (*Kollet and Zlontik, 2003; Cardenas and Zlontik, 2003*) have shown the absence of such a distinct interface between surface and subsurface.

New Overland Flow Boundary

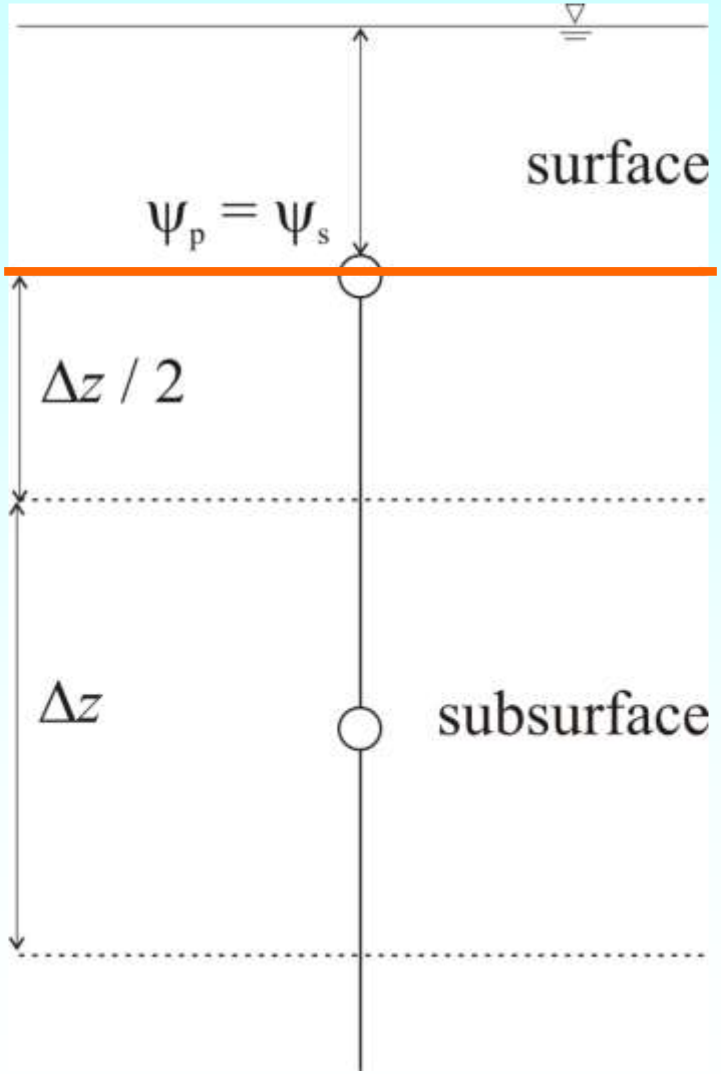

$$-k(x)k_r\nabla(\psi - z) = -\frac{\partial\|\psi,0\|}{\partial t} + \nabla\vec{v}\|\psi,0\| - q_s$$

$$S_s S_w \frac{\partial\psi}{\partial t} + \phi\frac{\partial S_w(\psi)}{\partial t} = \nabla\cdot q + q_g$$

Continuity conditions of pressure head and flux

$$\psi_s = \psi_p = h$$

$$q_{bc} = -k_{sz}k_r\nabla(\psi - z) = q_e$$

Kollet and Maxwell (2006)

Acronym	Year	Hydrologic Response		Sediment Transport	
		Surface	Subsurface	Channel	Overland
WEPP	1989	1D	n/a	1D	1D
ANSWERS	1980	2D	n/a	2D	2D
CREAMS	1980	1D	1D, C	n/a	1D
KINEROS2	1990	1D	n/a	1D	1D
EUROSEM	1998	3D	n/a	1D	1D
CASC2D	2000	2D	n/a	1D	2D
GSTARS4	2003	2D	n/a	1D	2D
SHESED	1996	2D	1D, U; 2D, S	1D	2D
InHm	2006	2D	3D, U/S	2D	2D
U (unsaturated); S (saturated); U/S (unsaturated/saturated); C (capacity approach)					

Comparison of selected models that consider both hydrologic response and sediment transport

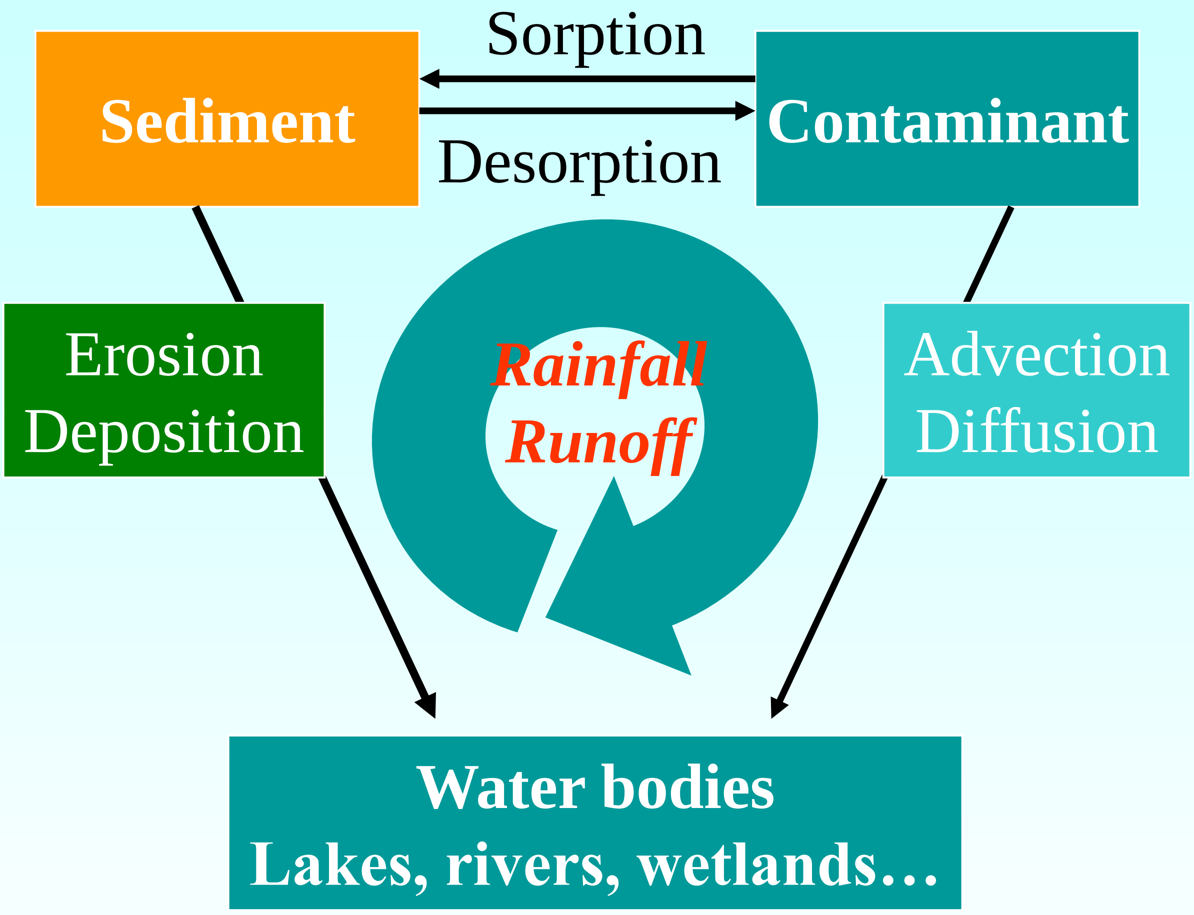

CREAMS; PRZM; GLEAMS; LEACHM; AGNPS; HSPF; HYDRUS-1D/2D; QUAL2E; WASP5/WASP6; HEM3D; RIVWQ

Coupled Contaminant Transport Modeling

- **A step towards integration of surface and subsurface processes was presented by *Govindaraju* (1996), who, by matching boundary conditions, could couple two-dimensional variably-saturated subsurface flow and transport with one-dimensional flow and transport on the land surface.**

- **First-order exchange coefficients are well established to couple transport in dual subsurface continua**

  e.g. ***van Genuchten and Wierenga, 1976;***
  Gerke and van Genuchten, 1993a & b, 1996;
  VanderKwaak Loague, 2001.

- **Although these models consider the solute transport processes in surface and subsurface domains, they ignored interactions between the dissolved contaminants in flow and adsorbed contaminants on the eroded soil particles due to sorption and desorption.**

Coupled Contaminant Transport Modeling

Due to the natural intrinsic connection between surface and subsurface waters, modeling of flow, soil erosion and transport, and contaminant transport should be considered as an integrated system.

Therefore, a generalized modeling framework considering the transport of both water-borne and sediment-borne contaminants in integrated surface/subsurface systems is established in this study.

RESEARCH OBJECTIVES

1. Coupled Surface-Subsurface Flow Model:

- **A new form of depth-averaged 2-D diffusion-wave surface flow equation, which does not rely on the traditional conductance concept.**
- **3-D unsteady variably saturated subsurface flow.**
- **Continuity conditions of pressure head and exchange flux are used at the ground surface.**

2. Soil Erosion and Transport Model:

- **The concept of nonequilibrium to facilitate the simulation of both erosion and deposition.**
- **Nonuniform total-load sediment transport is simulated.**
- **Detachment from rainsplash and/or hydraulic erosion driven by spatially variable surface flow.**

3. Coupled Surface-Subsurface Contaminant Transport Model:

- **Advection-diffusion (or -dispersion) equations.**
- **Sediment sorption and desorption of contaminants.**
- **Contaminant exchanges between surface and subsurface due to infiltration, diffusion, and bed change.**

4. Numerical Method:

Implicit finite volume method; SIP solver; Modified Picard procedure; Under-relaxation.

Flow Model — Governing Equations

Variably Saturated Subsurface Flow

$$\Theta S_s \frac{\partial H}{\partial t} + \frac{\partial \theta}{\partial t} = \frac{\partial}{\partial x}\left[K_x(\psi)\frac{\partial H}{\partial x}\right] + \frac{\partial}{\partial y}\left[K_y(\psi)\frac{\partial H}{\partial y}\right] + \frac{\partial}{\partial z}\left[K_z(\psi)\frac{\partial H}{\partial z}\right] + q_g$$

- H total head for subsurface flow
- Θ saturation of the soil
- θ volumetric soil water content
- S_s specific storage
- K_x K_y K_z hydraulic properties for unsaturated/saturated soil
- $K_i(\psi) = k_{si} k_{ri}(\psi)$
- k_s saturated hydraulic conductivity
- k_r relative permeability
- q_g general source and/or sink water terms

Note that this parabolic equation is highly nonlinear due to the nature of the hydraulic properties of soil layer and soil water content

Surface Flow

$$\frac{\partial H}{\partial t} = \frac{\partial}{\partial x}\left(k_{ox}\frac{\partial H}{\partial x}\right) + \frac{\partial}{\partial y}\left(k_{oy}\frac{\partial H}{\partial y}\right) + q_o + q_r + q_e$$

H water surface elevation, which is the sum of water depth ***h*** and bed elevation z_o

q_r rainfall rate; q_e water exchange rate with subsurface;

q_o other sources/sinks;

k_{ox}, k_{oy} diffusion coefficients, determined by $k_{ox} = \frac{h^{5/3}}{n_x^2 \Phi^{1/2}}$ and $k_{oy} = \frac{h^{5/3}}{n_y^2 \Phi^{1/2}}$

Φ friction or energy slope operator:

$$\Phi = \left[\left(\frac{\partial H}{\partial x}\right)^2 \frac{1}{n_x^4} + \left(\frac{\partial H}{\partial y}\right)^2 \frac{1}{n_y^4} \right]^{1/2}$$

Interactions between Surface and Subsurface

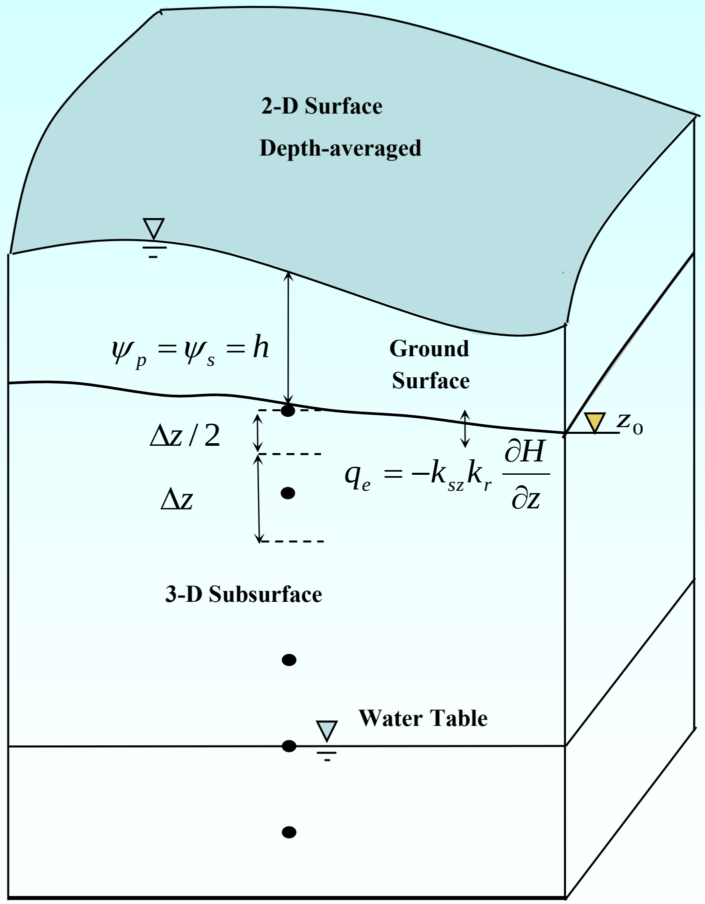

$$q_e = \frac{\partial \|H, z_0\|}{\partial t} - \frac{\partial}{\partial x}\left(k_{ox} \frac{\partial \|H, z_0\|}{\partial x}\right) - \frac{\partial}{\partial y}\left(k_{oy} \frac{\partial \|H, z_0\|}{\partial y}\right) - q_o - q_r$$

$$q_{bc} = -k_{sz} k_r \frac{\partial H}{\partial z} = -K_z \frac{\partial H}{\partial z} = q_e$$

$$-K_z \frac{\partial H}{\partial z} = \frac{\partial \|H, z_0\|}{\partial t} - \frac{\partial}{\partial x}\left(k_{ox} \frac{\partial \|H, z_0\|}{\partial x}\right) - \frac{\partial}{\partial y}\left(k_{oy} \frac{\partial \|H, z_0\|}{\partial y}\right) - q_o - q_r$$

$$\Theta S_s \frac{\partial H}{\partial t} + \frac{\partial \theta}{\partial t} = \nabla \cdot K(\psi) \nabla H + q_g$$

Flow Model — Boundary Conditions

The often used boundary conditions:

Dirichlet type: prescribed head

Neuman type: prescribed flux

Impervious boundary or a no-flow boundary is a special case of the Neuman boundary condition in which the normal flux is zero.

Boundary conditions for surface flow:

Zero-depth-gradient (ZDG) $q_{ZDG} = \frac{h^{5/3}}{n}\sqrt{S_0}$

Critical depth (CD) $q_{CD} = \sqrt{gh^3}$

Numerical Solutions

Finite Volume Method

Fully Implicit

Modified Picard Procedure

SIP Solver

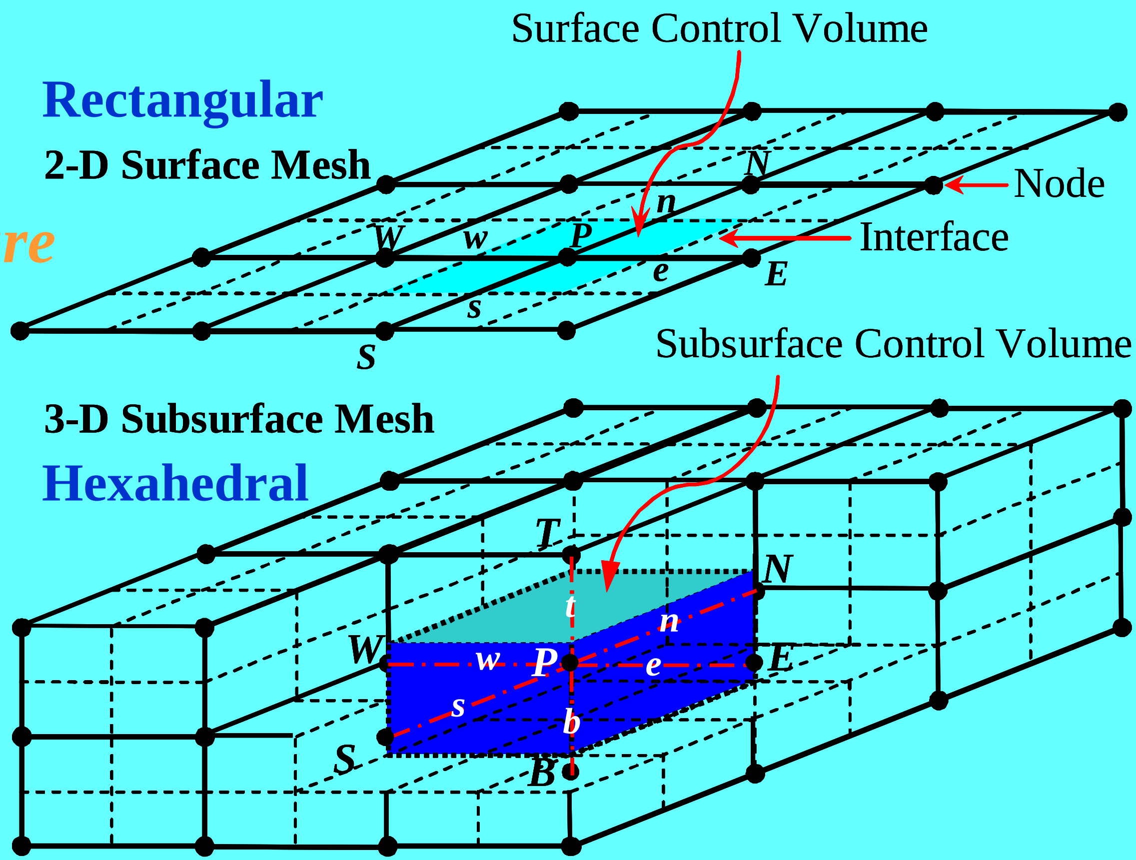

Derivative term of moisture content:

$$\theta_i^{n+1,m+1} \approx \theta_i^{n+1,m} + \left.\frac{\partial \theta}{\partial \psi}\right|^{n+1,m} \left(H^{n+1,m+1} - H^{n+1,m}\right)$$

Upwind scheme:

$$k_{ox,e}^{n+1,m} = \beta \cdot k_{ox,P}^{n+1,m} + (1-\beta) \cdot k_{ox,E}^{n+1,m} \qquad \begin{cases} \beta = 1 & q_P > 0 \\ \beta = 0 & q_P < 0 \end{cases}$$

$$\Phi_P^{n+1,m+1} = Max\left\{\varepsilon, \Phi_P^{n+1,m}\right\}$$

Solution Procedure of Flow Model

Flow calculations are executed in the following sequence:

1) Read input data and initial variables;
2) Call surface flow subroutine to solve Eq. (3.1.26);
3) Call subsurface flow subroutine to solve Eq. (3.1.8);
4) Determine if the convergence criterion

$$\left| \frac{H_i^{n+1,m+1} - H_i^{n+1,m}}{H_i^{n+1,m}} \right| < \varepsilon$$

is satisfied.
If not, return to step 2) for next iteration step.
If yes, go to step 5);

5) Update computational time and return to step 2) for next time step until a specified time is reached.

2-D Upland Soil Erosion and Transport Model

Nonequilibrium concept:

In soil erosion and transport on overland flow areas, detachment and deposition may occur simultaneously, and the sediment concentration is determined by the relative magnitude of these two processes.

2-D depth-averaged nonuniform sediment transport equation

$$\frac{\partial(hC_{tk})}{\partial t}+\frac{\partial(uhC_{tk})}{\partial x}+\frac{\partial(vhC_{tk})}{\partial y}=\frac{\partial}{\partial x}\left(\varepsilon_s h\frac{\partial C_{tk}}{\partial x}\right)+\frac{\partial}{\partial y}\left(\varepsilon_s h\frac{\partial C_{tk}}{\partial y}\right)+E_{sed,k}$$

Bed change is determined by

$$(1-\lambda)\rho_s\left(\frac{\partial z_b}{\partial t}\right)_k=-E_{sed,k}$$

Total soil erosion rate:

$$E_{sed,k}=D_{ik}+D_{fk}$$

Interrill erosion

Rill erosion

2-D Upland Soil Erosion and Transport Model

Interrill erosion **depends on**

soil and slope characteristics, vegetation and land use, rainfall intensity, and hydraulic factors of runoff.

RUSLE2	$D_{ik} = 0.5 r K S_i C p_c p_{bk}$
WEPP	$D_{ik} = K_{iadj} i_e \sigma_{ir} SDR_{RR} F_{nozzle} \frac{R_s}{Wid} p_{bk}$
Jain et al. (2005)	$D_{ik} = p_{bk} \omega F_w C K i^a \left(2.96 S_0^{0.79} + 0.56\right) / \rho_s$ $F_w = \begin{cases} \exp\left(1 - h / D_m\right) & if \quad h > D_m \\ 1 & if \quad h < D_m \end{cases}$
Liu et al.(2006)	$\frac{D_{ik} d}{R_c} = 1.8 \times 10^{-9} \left(\frac{h}{d}\right)^{1.5} \left(1.05 - 0.85 e^{-4 S_0}\right) p_{bk}$ $R_c = \frac{6.42}{(s-1)^{0.5}} \left(Y - Y_c\right) d S_f^{0.6} u \rho_s$

2-D Upland Soil Erosion and Transport Model

Rill erosion **based on the nonequilibrium concept**

$$D_{fk} = \frac{1}{L}\left(T_{ck} - q_{sk}\right)$$

L **is the adaptation length, which is the characteristic distance that the sediment concentration of rill flow re-establishes from a nonequilibrium state to the equilibrium state:**

$$L = uh/\left(\alpha_t \omega_{sk}\right)$$ **(Wu, 2004)**

Numerical Methods for Sediment Model

$$\frac{\partial(hC_{tk})}{\partial t}+\frac{\partial}{\partial x}\left(uhC_{tk}-\varepsilon_s h\frac{\partial C_{tk}}{\partial x}\right)+\frac{\partial}{\partial y}\left(vhC_{tk}-\varepsilon_s h\frac{\partial C_{tk}}{\partial y}\right)=E_{sed,k}$$

Implicit FVM ↓ ***Exponential scheme***

Finial discretized sediment transport equation:

$$\frac{h_P^{n+1}C_{tk,P}^{n+1}-h_P^n C_{tk,P}^n}{\Delta t}\Delta A_P=\sum^{i=E,W,N,S} a_i^C C_{tk,i}^{n+1}-a_P^C C_{tk,P}^{n+1}+E_{sed,k}\Delta A_P$$

e.g. $a_E^C=\frac{F_e}{\exp(F_e/D_e)-1}$ $\quad a_P^C=a_E^C+a_W^C+a_N^C+a_S^C+F_e-F_w+F_n-F_s$

Bed change equation $\quad \Delta Z_{bk,P}^{n+1}=-\frac{\Delta t}{(1-\lambda)\rho_s}E_{sed,k}$

Bed elevation is then updated as $\quad z_{b,P}^{n+1}=z_{b,P}^n+\Delta z_{b,P}^{n+1}$

Bed material sorting

$$p_{bk,P}^{n+1}=\frac{\Delta z_{bk,P}^{n+1}+\delta_{m,P}^n p_{bk,P}^n+p_{bk,P}^{*,n}\left(\delta_{m,P}^{n+1}-\delta_{m,P}^n-z_{b,P}^{n+1}\right)}{\delta_{m,P}^{n+1}}$$

Coupled Surface-Subsurface Model for Contaminant Transport

General form: $$\frac{DC_i}{Dt} = S_c$$

For the depth-averaged 2-D surface flow

$$\frac{DC}{Dt} = \frac{1}{h}\left[\frac{\partial(hC)}{\partial t} + \frac{\partial}{\partial x}\left(uhC - E_x h\frac{\partial C}{\partial x}\right) + \frac{\partial}{\partial y}\left(vhC - E_y h\frac{\partial C}{\partial y}\right)\right]$$

For 3-D variably saturated subsurface flow

$$\frac{DC}{Dt} = \frac{\partial(\lambda\Theta C)}{\partial t} + \frac{\partial}{\partial x}\left(uC - \lambda\Theta D_x\frac{\partial C}{\partial x}\right) + \frac{\partial}{\partial y}\left(vC - \lambda\Theta D_y\frac{\partial C}{\partial y}\right)$$

$$+ \frac{\partial}{\partial z}\left(wC - \lambda\Theta D_z\frac{\partial C}{\partial z}\right)$$

$$(u_i = \lambda\Theta v_i)$$

Sorption and Desorption of Contaminants on Sediment

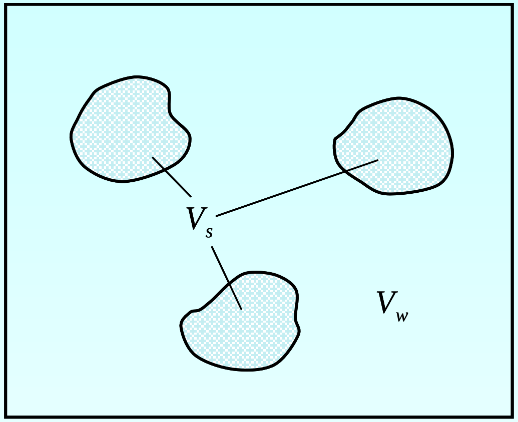

Concentrations of dissolved and adsorbed parts:

$$C_d = \frac{M_d}{V_t} \qquad C_s = \frac{M_s}{V_t}$$

Total contaminant concentration:

$$C_t = C_d + C_s = \frac{M_d + M_s}{V_t}$$

Linear isotherm

$$R_{ad} = k_{ad}\rho_s S \frac{C_d}{1-S} = k_{ad} r_{sw} C_d$$

$$R_{de} = k_{de} C_s$$

Equilibrium partition

$$\frac{C_s}{C_d} = \frac{k_{ad} r_{sw}}{k_{de}} = k_D r_{sw}$$

In fact, other models, such as the Langmuir isotherm and Freundlich isotherm, are also commonly used.

Contaminant Transport in Surface /Subsurface Flows

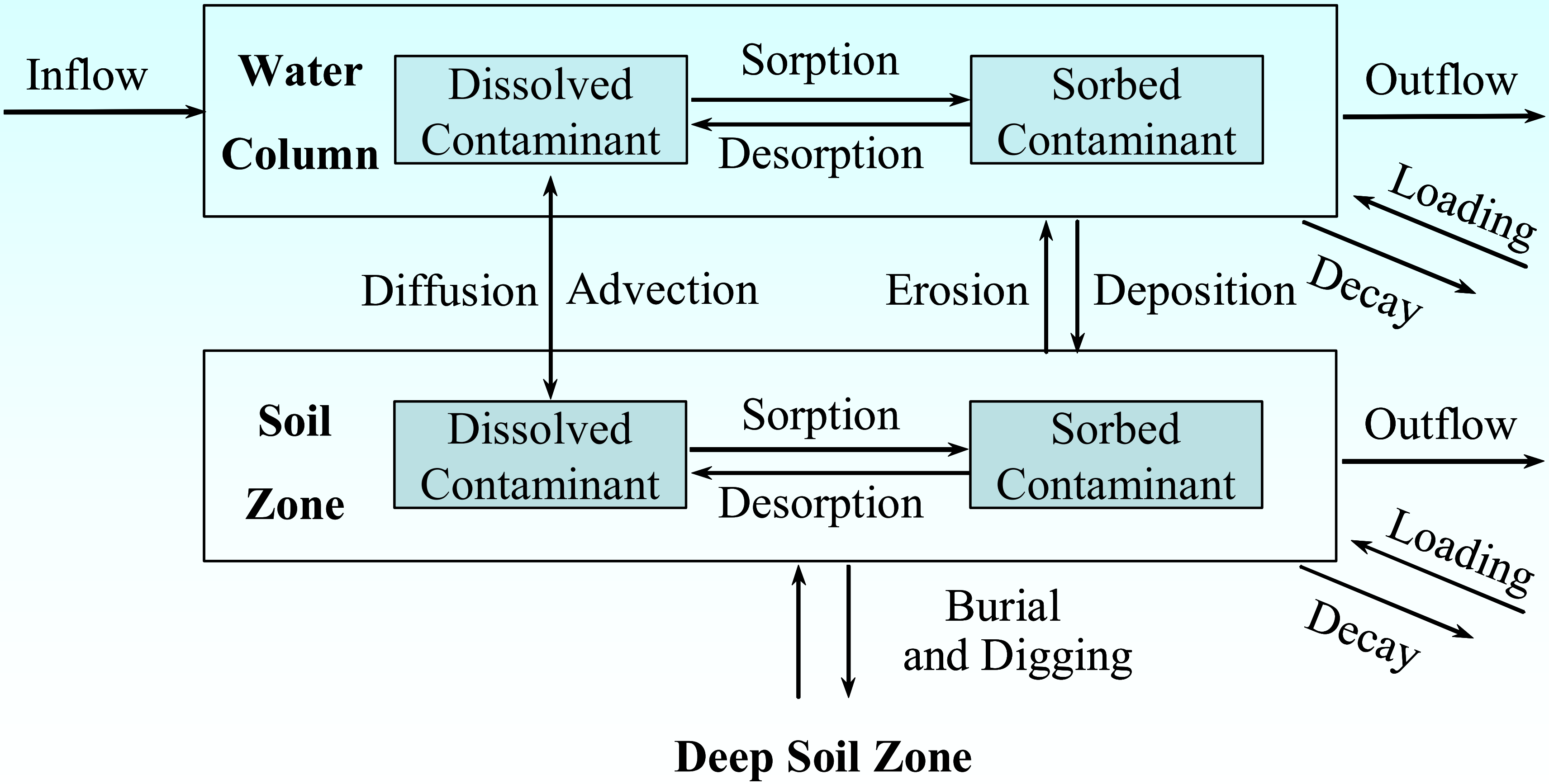

Exchanges of Contaminant between Surface and Subsurface

Mass exchange of dissolved contaminant at the bed surface:

$$q_{dwg,ex} = q_e C_{de} + k_{dwg}\left(\frac{C_{dg}}{\theta} - \frac{C_{dw}}{1-S}\right) \rightarrow q_{twg,ex} = q_e f_{de} C_{te} + k_{dwg}\left(\frac{f_{dg}}{\theta} C_{tg} - \frac{f_{dw}}{1-S} C_{tw}\right)$$

Mass exchange coefficient

Wallach et al. (1988, 1989)

Exchange due to sediment erosion and deposition:

$$q_{s,ex} = \max\left(D_{fk},0\right)\frac{C_{sg}}{(1-\lambda)\rho_s} + D_{ik}\frac{C_{sg}}{(1-\lambda)\rho_s} + \min\left(D_{fk},0\right)\frac{C_{sw}}{\rho_s S}$$

$$q_{d,ex} = \max\left(D_{fk},0\right)\frac{C_{dg}}{(1-\lambda)\rho_s} + D_{ik}\frac{C_{dg}}{(1-\lambda)\rho_s} + \min\left(D_{fk},0\right)\frac{\theta}{(1-\lambda)\rho_s}\frac{C_{dw}}{1-S}$$

$$q_{t,ex} = \max\left(D_{fk},0\right)\frac{C_{tg}}{(1-\lambda)\rho_s} + D_{ik}\frac{C_{tg}}{(1-\lambda)\rho_s} + \min\left(D_{fk},0\right)\left[\frac{\theta}{(1-\lambda)\rho_s}\frac{f_{dw}}{1-S} + \frac{f_{sw}}{\rho_s S}\right]C_{tw}$$

Contaminant in Surface and Subsurface

Dissolution of contaminant

Solubility of contaminant

$$q_{sol} = k_{sol}(C_{sol} - C_a)$$

Surface mass transfer coefficient, related to the aqueous phase diffusion coefficient

Decay of contaminant

$$q_{decay} = -k\ C$$

by volatilization, photolysis, hydrolysis, biodegradation, and chemical reactions

Contaminant Transport in Surface Flow

Nonequilibrium Partition Model:

$$\frac{DC_{dw}}{Dt} = \frac{J_{d,aw}}{h} + q_{dw} - k_{ad,w} r_{sw,w} C_{dw} + k_{de,w} C_{sw} - k_{dw} C_{dw} + \frac{q_{dwg,ex}}{h} + \frac{q_{d,ex}}{h}$$

$$\frac{DC_{sw}}{Dt} = q_{sw} + k_{ad,w} r_{sw,w} C_{dw} - k_{de,w} C_{sw} - k_{sw} C_{sw} + \frac{q_{s,ex}}{h}$$

Equilibrium Partition Model:

$$\frac{DC_{tw}}{Dt} = \frac{J_{d,aw}}{h} + q_{tw} - k_{t,w} C_{tw} + \frac{q_{twg,ex}}{h} + \frac{q_{t,ex}}{h} + \frac{q_{sol}}{h}$$

Contaminant Transport in Subsurface Flow

Nonequilibrium Partition Model:

$$\frac{\partial\left(C_{dg}\right)}{\partial t}+\frac{\partial}{\partial x_i}\left[v_i C_{dg}-\theta D_{ij}\frac{\partial\left(C_{dg}/\theta\right)}{\partial x_i}\right]=-k_{ad,g}r_{sw,g}C_{dg}+k_{de,g}C_{sg}-k_{dg}C_{dg}+S_{dg}^{c}$$

$$\frac{\partial\left(C_{sg}\right)}{\partial t}=k_{ad,g}r_{sw,g}C_{dg}-k_{de,g}C_{sg}-k_{sg}C_{sg}+S_{sg}^{c}$$

Equilibrium Partition Model:

$$\frac{\partial\left(C_{tg}\right)}{\partial t}+\frac{\partial}{\partial x_i}\left[v_i f_{dg}C_{tg}-\theta D_{ij} f_{dg}\frac{\partial\left(C_{tg}/\theta\right)}{\partial x_i}\right]=-k_{tg}C_{tg}+S_{tg}^{c}$$

Subsurface Flow Simulation

Case 1. Comparison with analytical solution

Parameters: (Haverkamp et al., 1977)

Relative permeability	Water content	Moisture capacity	Initial condition	Boundary condition
$k_r(\psi) = \dfrac{A}{A + \lvert\psi\rvert^{\beta}}$	$\theta(\psi) = \dfrac{\alpha(\theta_s - \theta_r)}{\left(\alpha + \ln\lvert\psi\rvert^{\beta}\right)}$	$C(\psi) = \dfrac{\alpha\beta(\theta_s - \theta_r)\lvert\psi\rvert^{\beta-1}}{\psi\left(\alpha + \ln\lvert\psi\rvert^{\beta}\right)^2}$	$\theta_0 = 0.2376$ $t < 0, z \geq 0$	$\theta_1 = 0.4950$ $t \geq 0, z = 0$
Parameters: $A = 124.6, B = 1.77, \theta_s = 0.495, \theta_r = 0.124, \alpha = 739, \beta = 4, k_s = 4.428 \times 10^{-4}$ m/hr.				

Phillip, 1969:
A quasi-analytical solution for 1-D infiltration

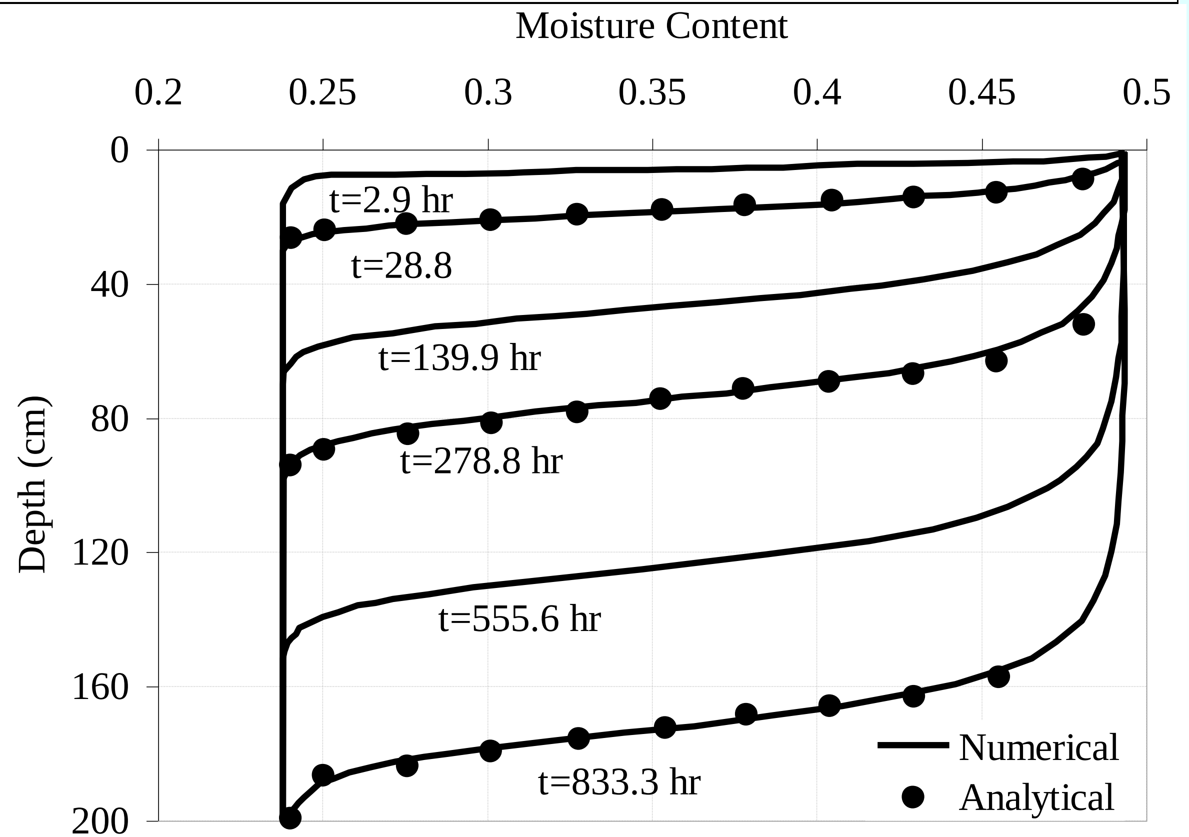

Case 2. Comparison with numerical solution of Zhang and Ewen (2000)

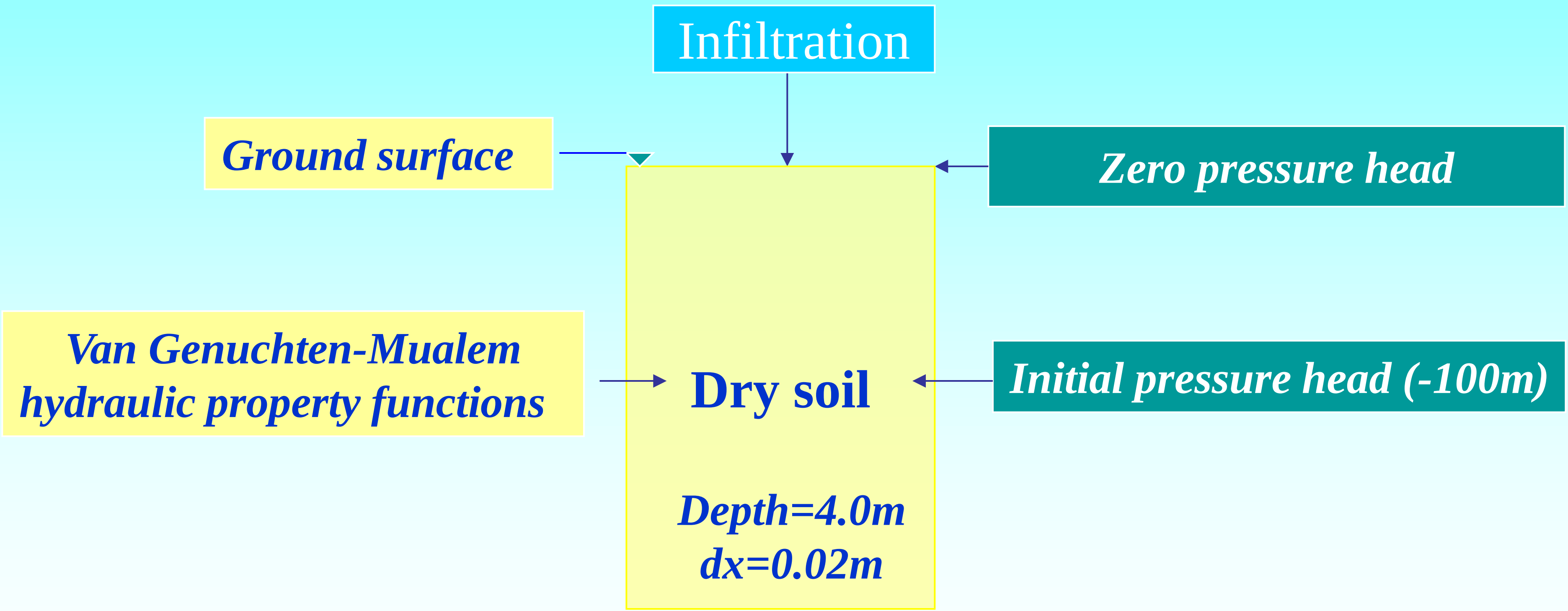

Parameters

$n = 3.45$ $\alpha = 1.5 m^{-1}$ $\theta_s = 0.45$ $\theta_r = 0.05$ $K_s = 0.8 m/d$

Case 2. Comparison with numerical solution

Results: after 1 day of infiltration

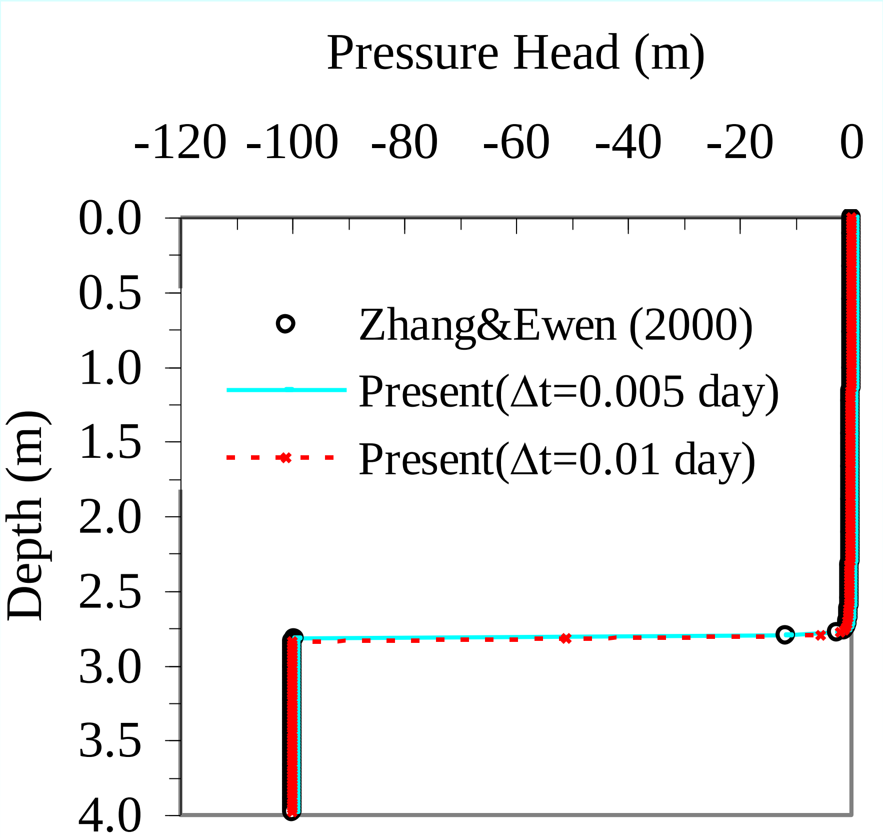

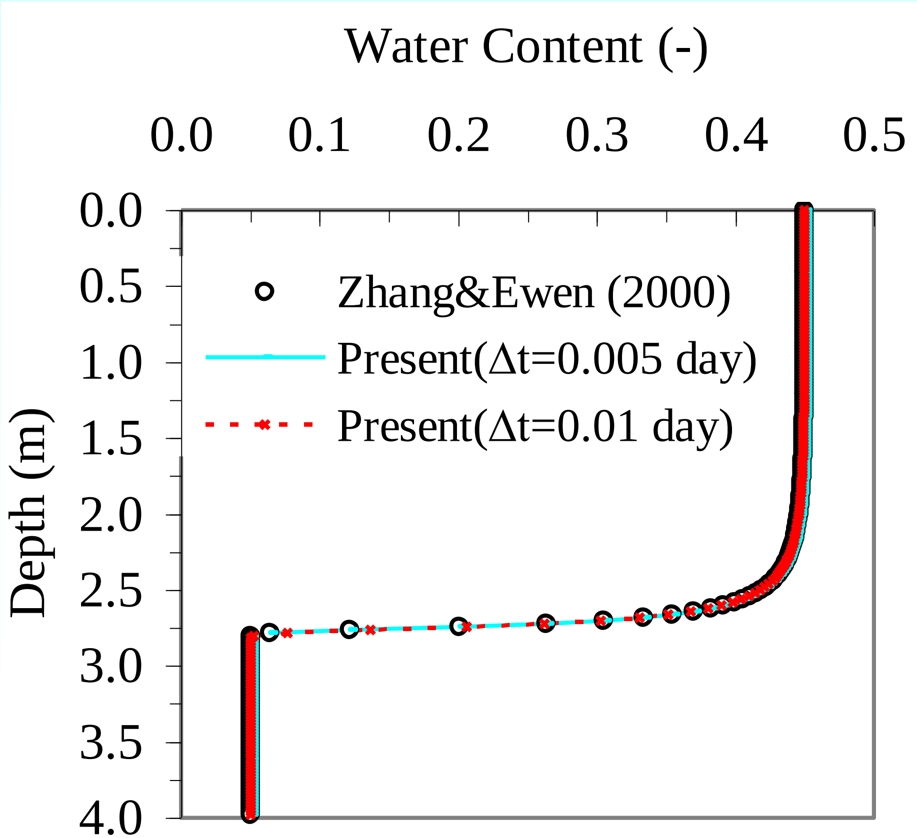

Surface Flow Simulation

Comparison with 1-D analytical solution

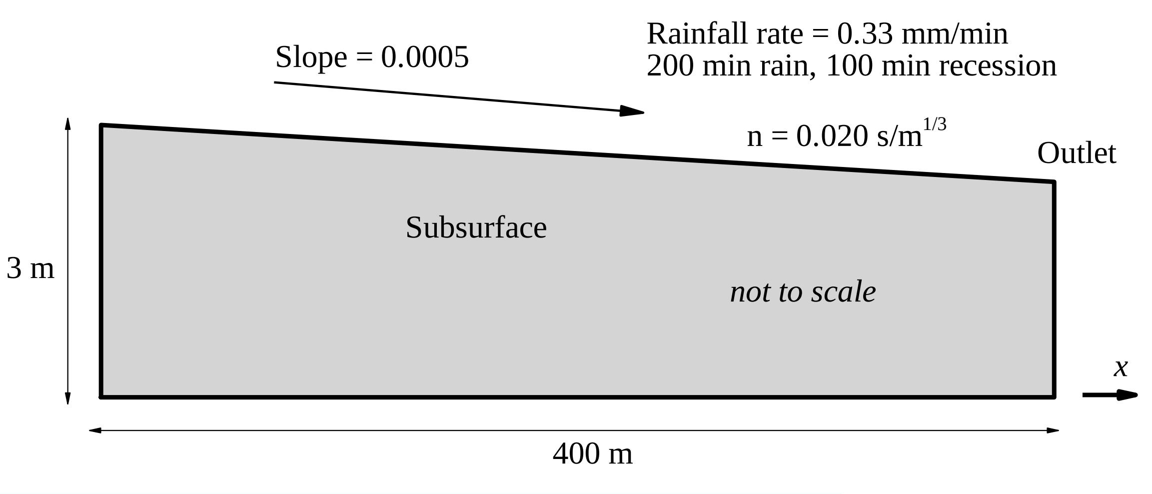

Gottardi and Venuttelli (1993)

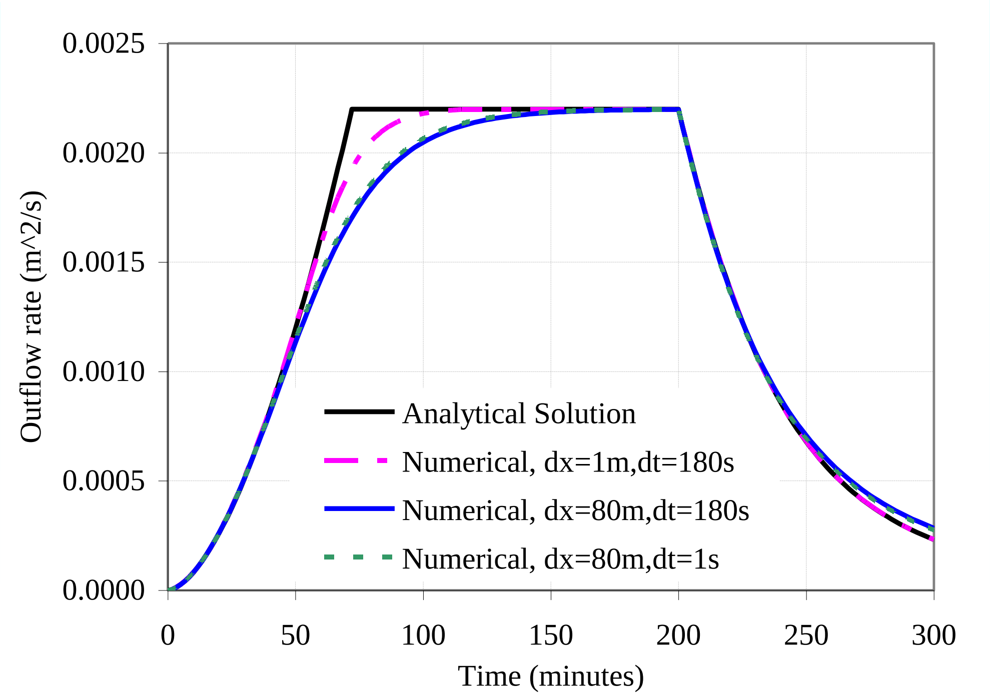

Overland flow over a 2-D V-catchment

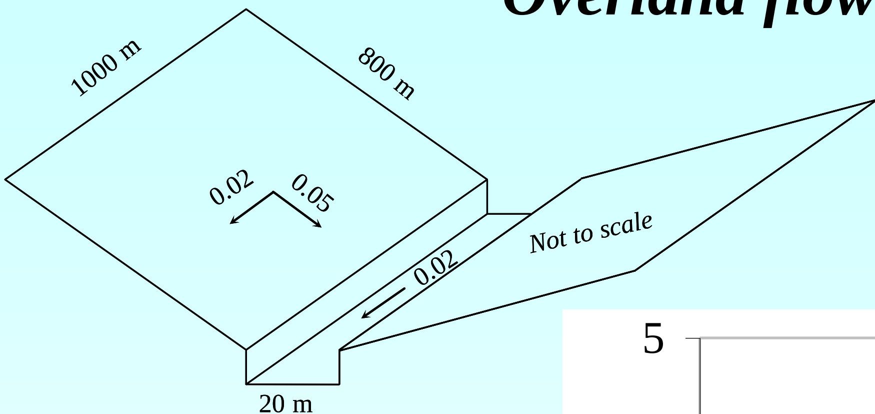

diGiammarco et al. (1996)

Panday and Huyakorn (2004)

Rainfall duration: 90 min

Rainfall intensity:

$$q_r = 3\times10^{-6}\ \text{m/s}$$

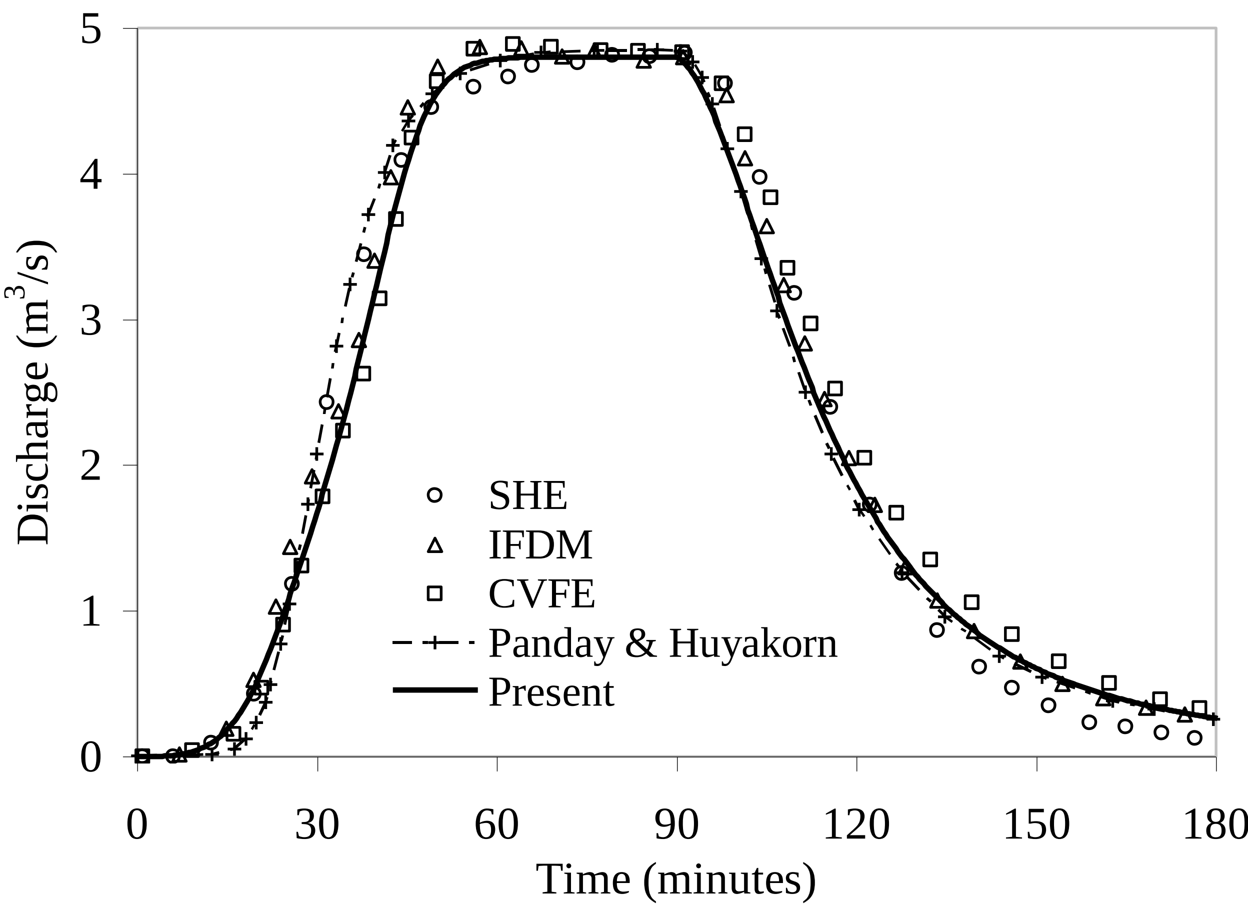

Coupled Flow Simulation

Test Case 1: *Experiment of Smith and Woolhiser (1971)*

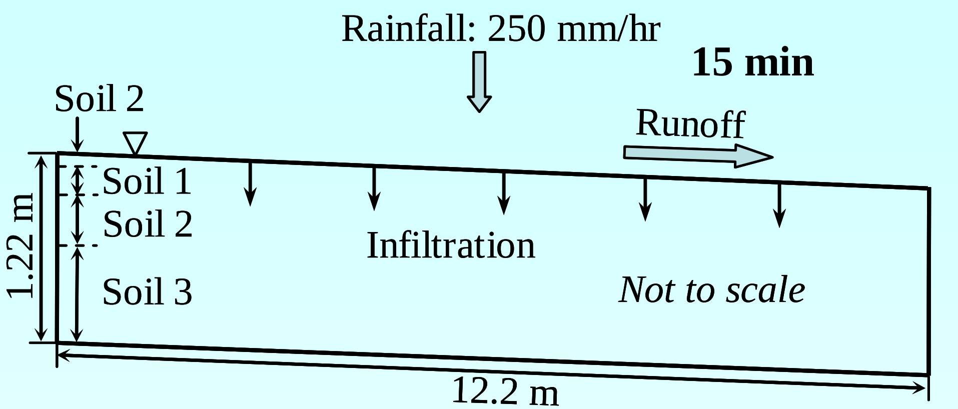

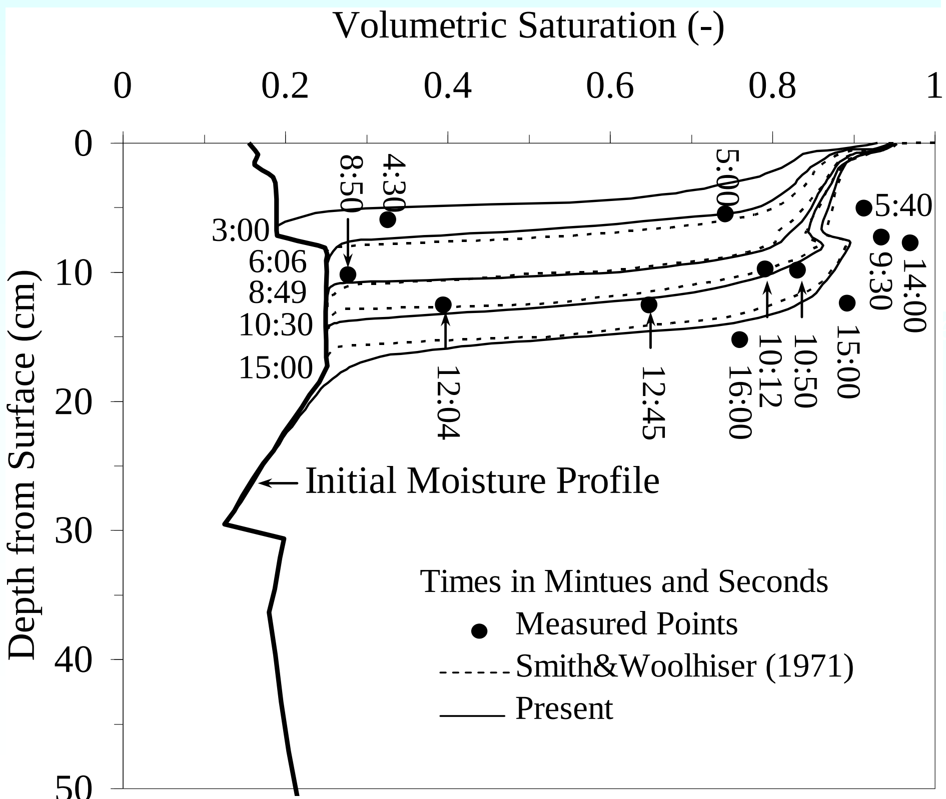

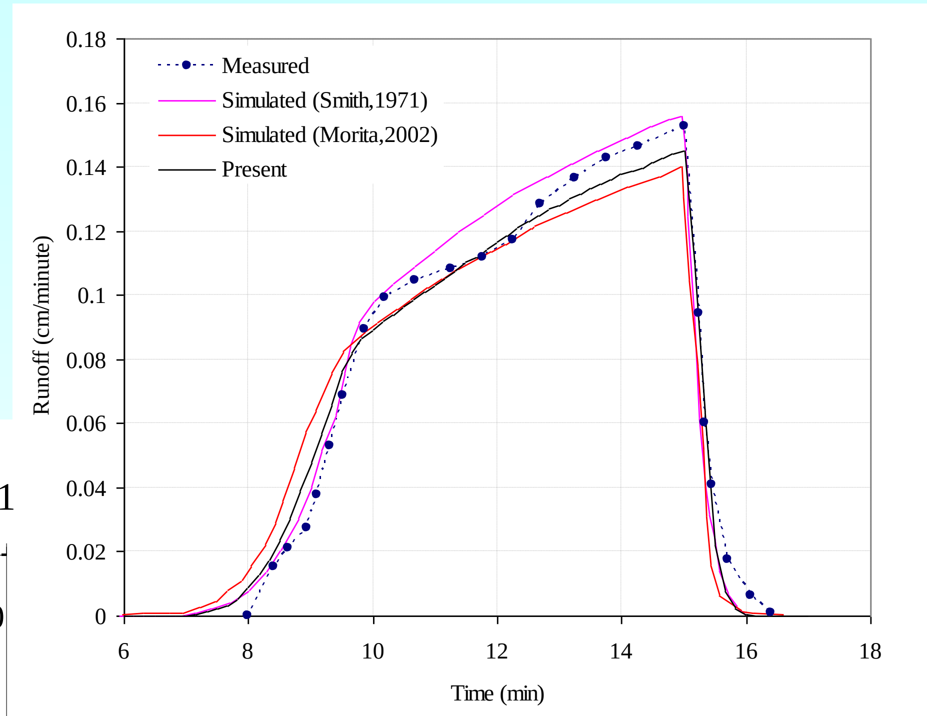

Coupled Flow Simulation

Case 2: Field-scale experiments by Abdul and Gillham (1989)

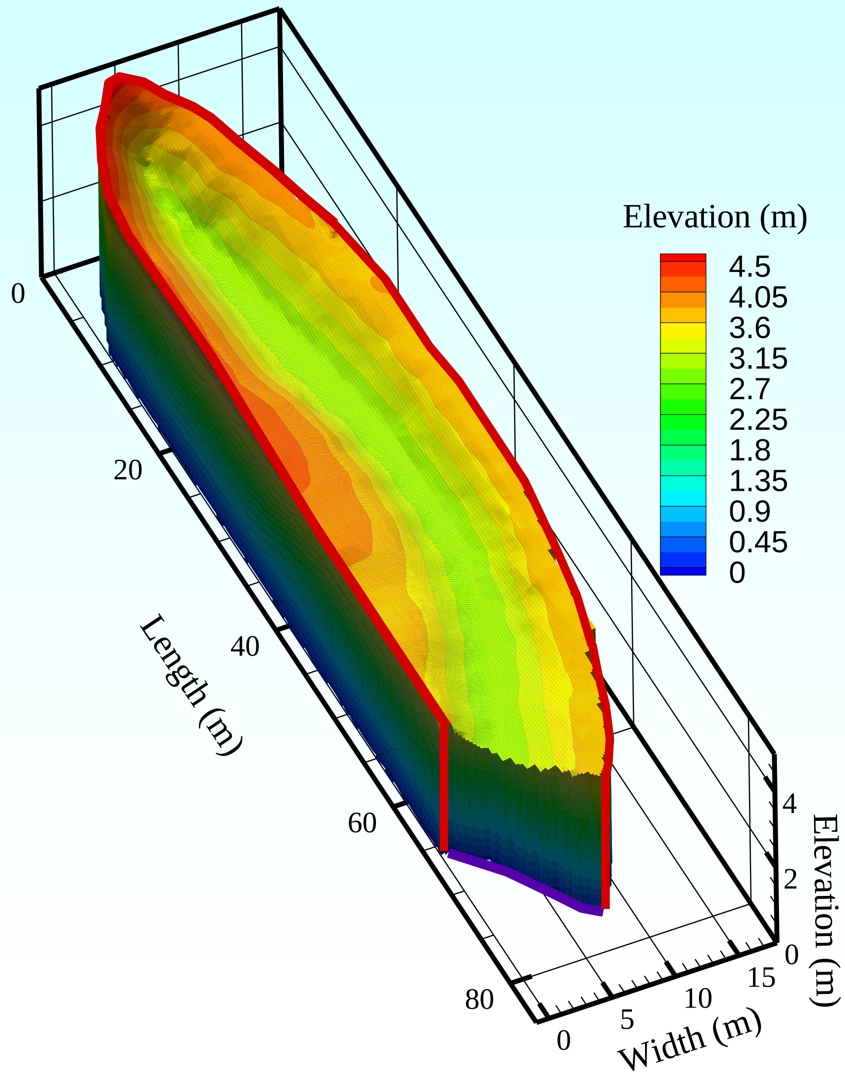

Location:

Toronto, Ontario, Canada

Size:

Grass-covered, 18 m × 80 m

Channel:

Grass-free, 60 cm wide

Subsurface:

Sandy layer, clayey silt, 4 m

Field-scale Experiment

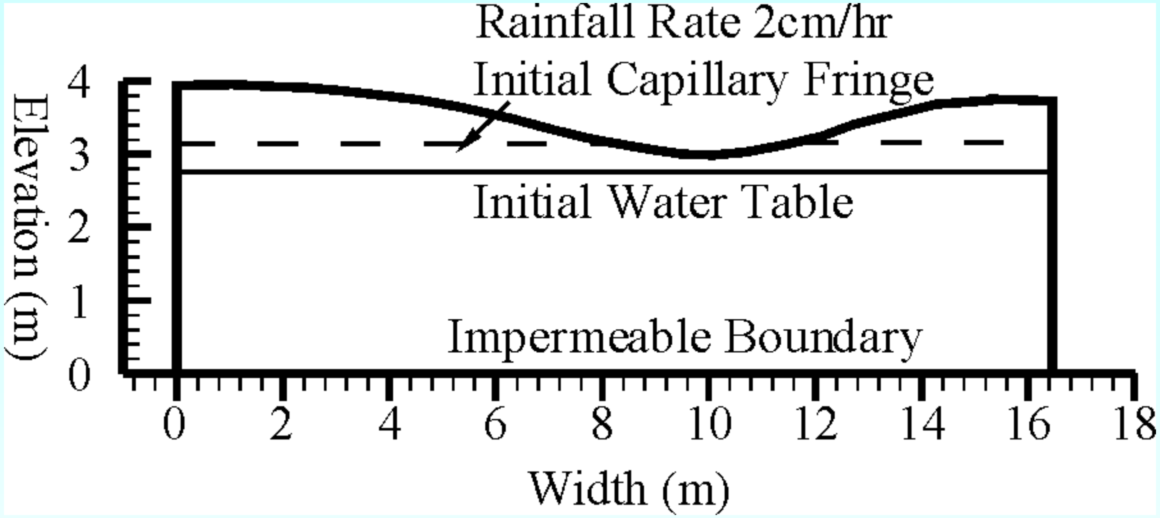

Initial and boundary conditions along a cross-section at *x*=40 *m*

Saturation-pressure head	Van Genuchten-Mualem Eqs. $\alpha = 1.9, n = 6$
Saturation-relative permeability	$k_{rw} = a(S_w n_e)^b \approx (S_w)^b$, $a = 110, b = 4.5$
Compressibility	$\beta_p = 3.3 \times 10^{-8} ms^2 / kg$
Initial total head	$H = \psi + z = 2.78m$
Channel roughness	$0.03 s / m^{1/3}$
Upland roughness	$0.3 s / m^{1/3}$

Coupled Surface/Subsurface Flow Simulation

Field-scale Experiment

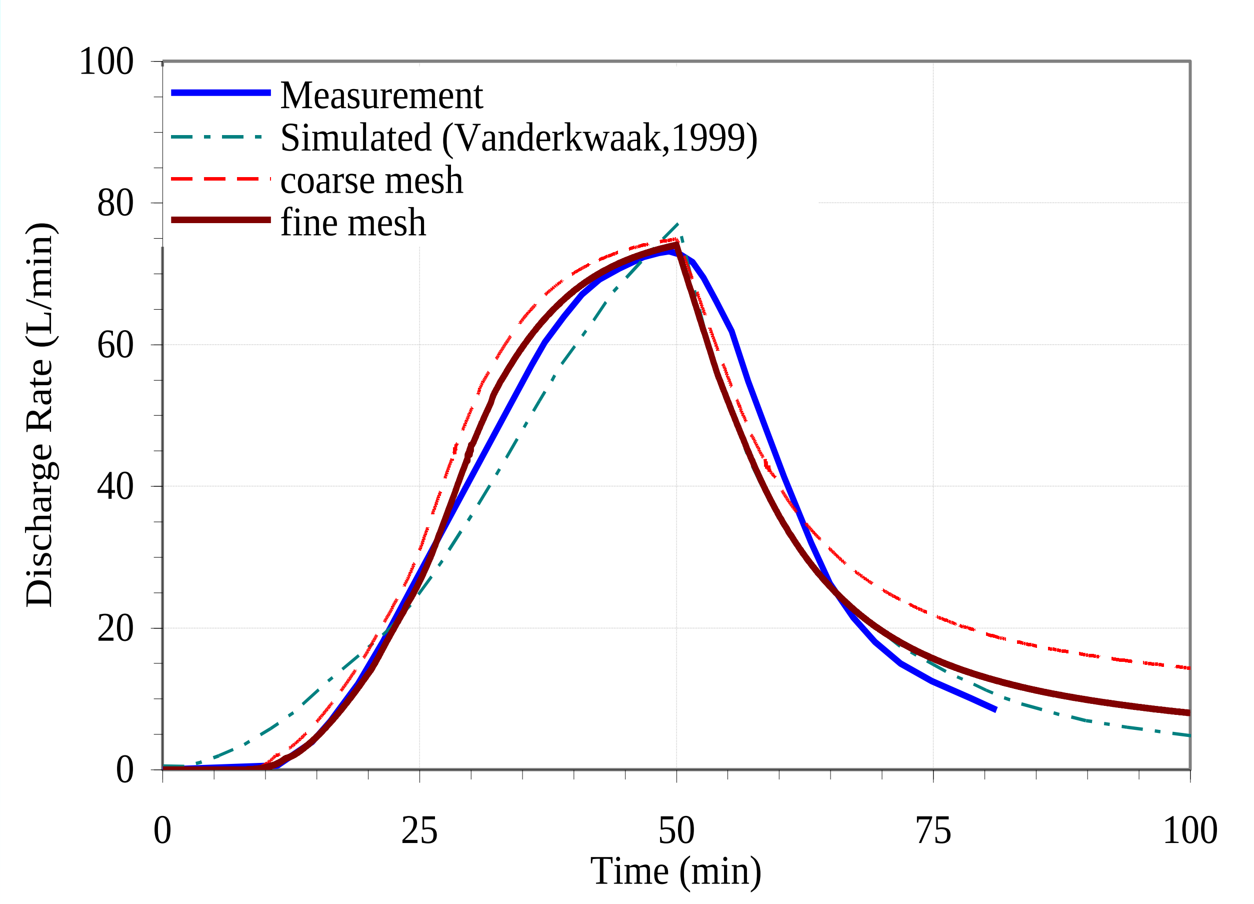

Comparison of measured and simulated stream discharges with time

Field-scale Experiment

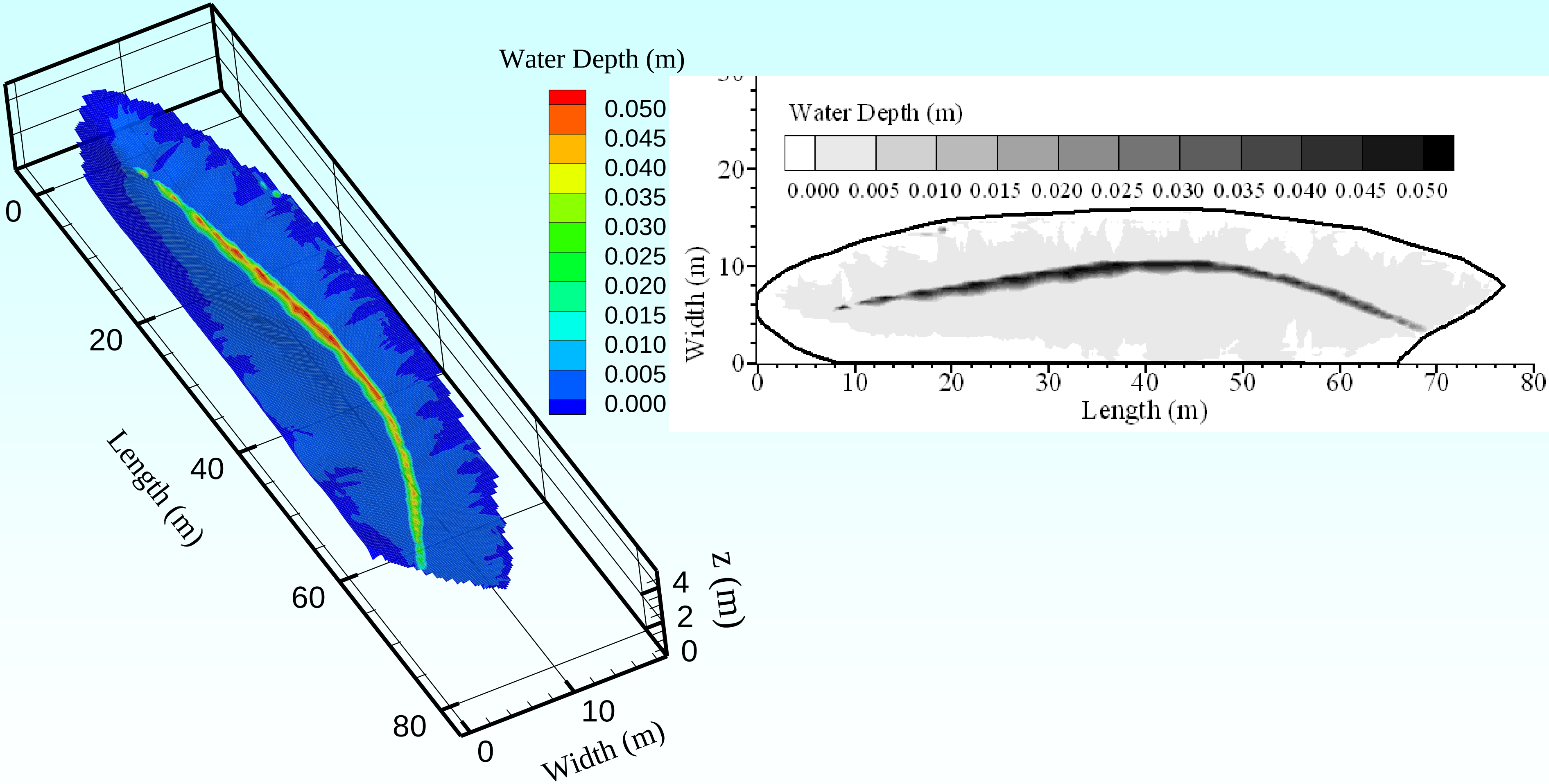

Water depth at 50 minutes

Verification of Soil Erosion and Transport Model

Case 1: Liu et al. (2006):
Test plot: 3.2 m × 1.0 m × 0.3 m
Wooden box with holes at the bottom.

Soil thickness: 25 cm; d_{50}=0.02 mm

Bulk density of soil	Initial moisture content	Saturated water content	Saturated hydraulic conductivity	Soil suction	Rainfall intensity		Slope	
					Run 1	Run 2	Run 1	Run 2
1.33 (g/cm^3)	0.2206 (-)	0.5027 (-)	1.6×10^{-6} (m/s)	0.15 (m)	2.06 (mm/min)	1.34 (mm/min)	15^o	20^o

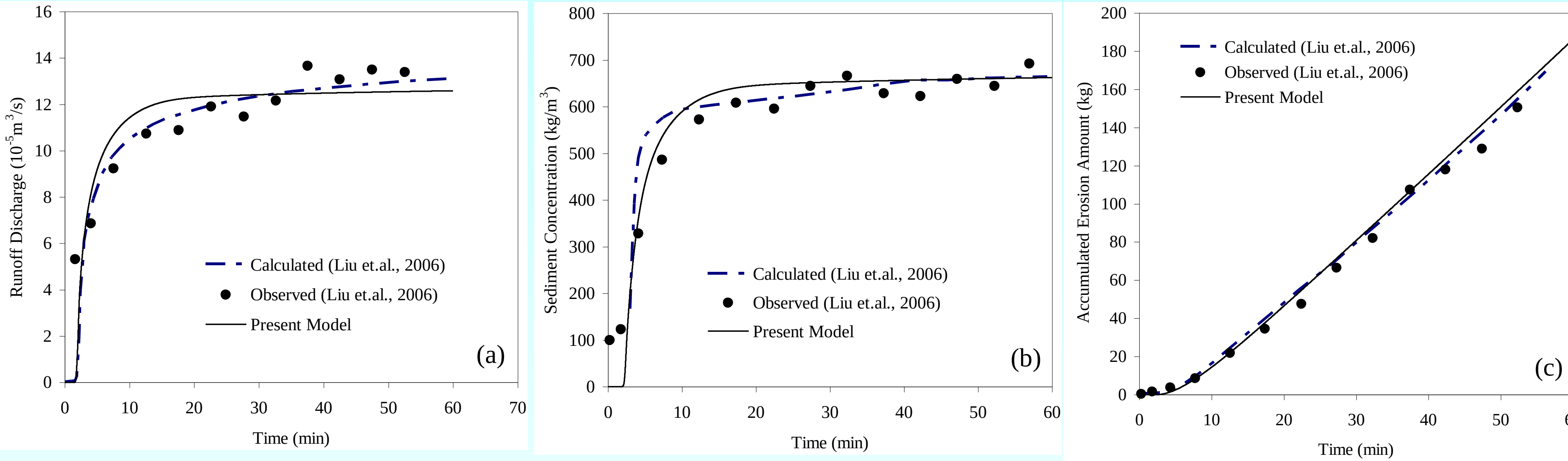

Run 1 (a) Runoff discharge, (b) Sediment concentration, (c) Accumulated erosion amount

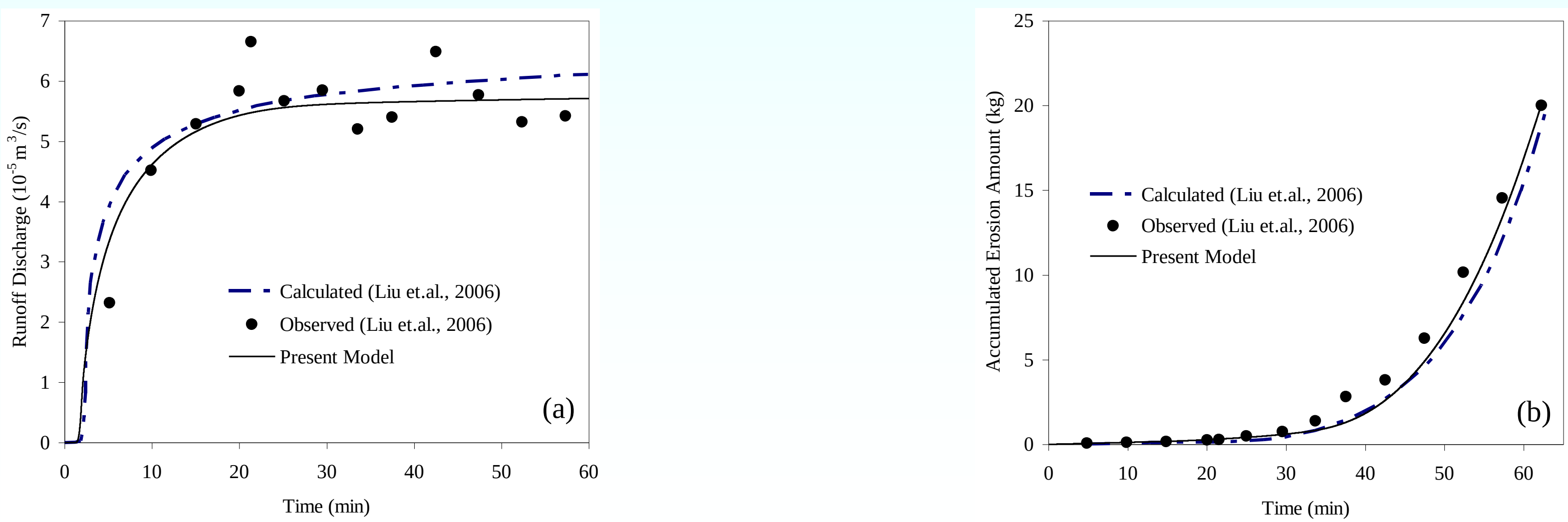

Run 2 (a) Runoff discharge, (b) Accumulated erosion amount

Case 2. Barfield et al. (1983)

Test plot: 4.6 m × 22.1 m; slope: 0.09

Conditions of experiments (Barfield et al., 1983)

Run No.	Bed material	Rainfall intensity (mm/hr)	Rainfall duration (min)	d_{50} (mm)	Soil erodibility factor K
P33131	Tilled & Wet topsoil	61	30	0.06	0.388
P33231		66			0.437

Manning coefficient and average infiltration rate (Yang and Shih, 2006)

Run	Manning coefficient	Average infiltration rate (mm/hr)
P33131	0.10	4.5
P33231	0.13	10.5

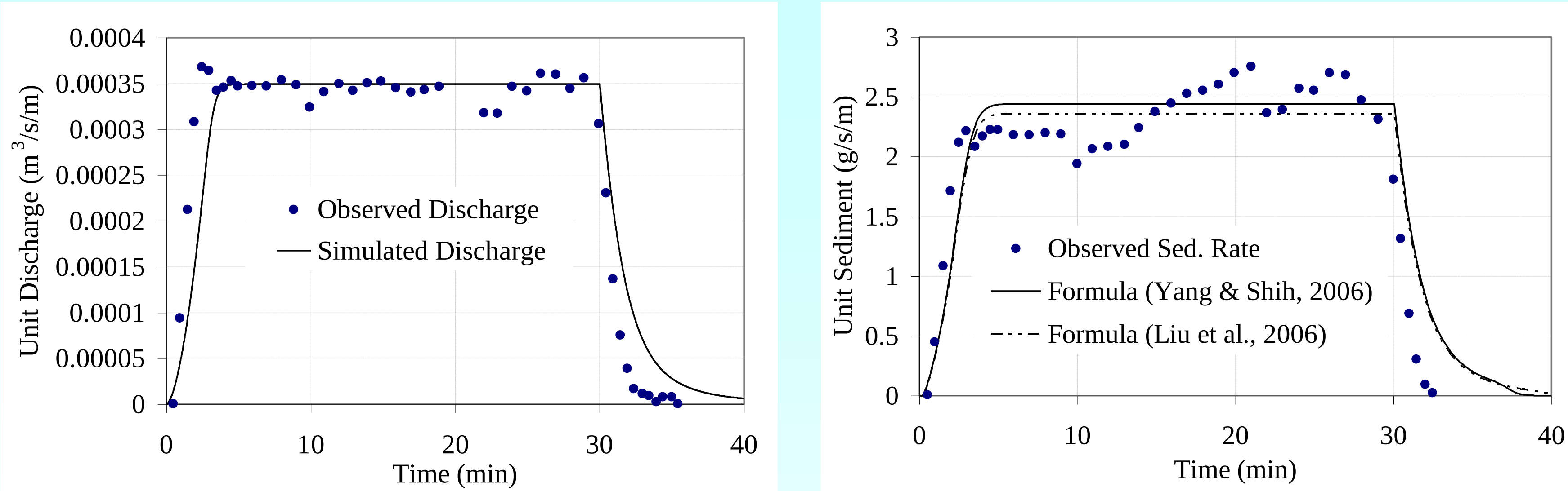

Flow and sediment discharges of run No. P33131

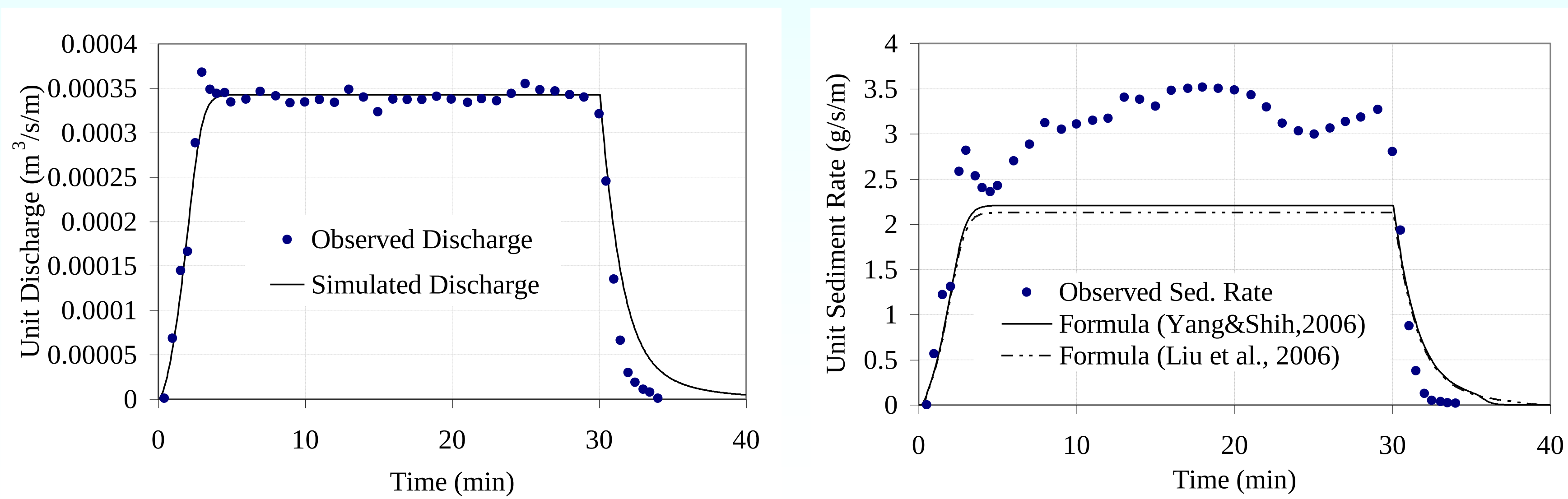

Flow and sediment discharges of run No. P33231

Verification of Contaminant Transport Model

Comparison with an Analytical Solution for Transport of Soil-released Chemical by Overland Flow (Rivlin and Wallach, 1995)

$$\frac{\partial(ch)}{\partial t} + \frac{\partial(uhc)}{\partial x} = k_{ch}\left(c_{soil} - c\right)$$

Parameters:
Rainfall: 1.6 cm/hr
Duration: 15 min
Infiltration: 0.3 cm/hr
k_{ch} = 0.9 cm/hr

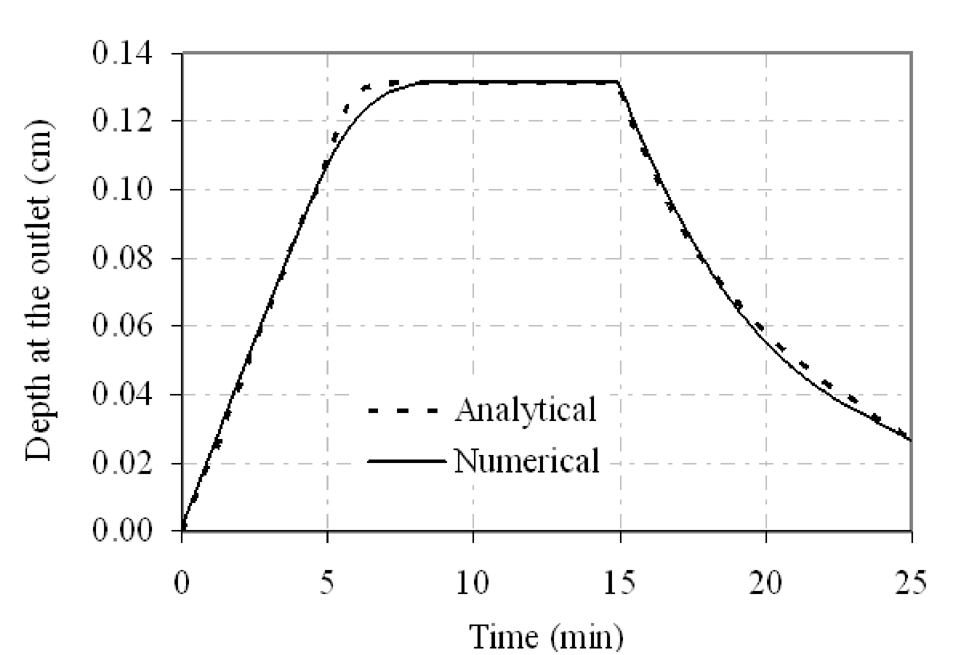

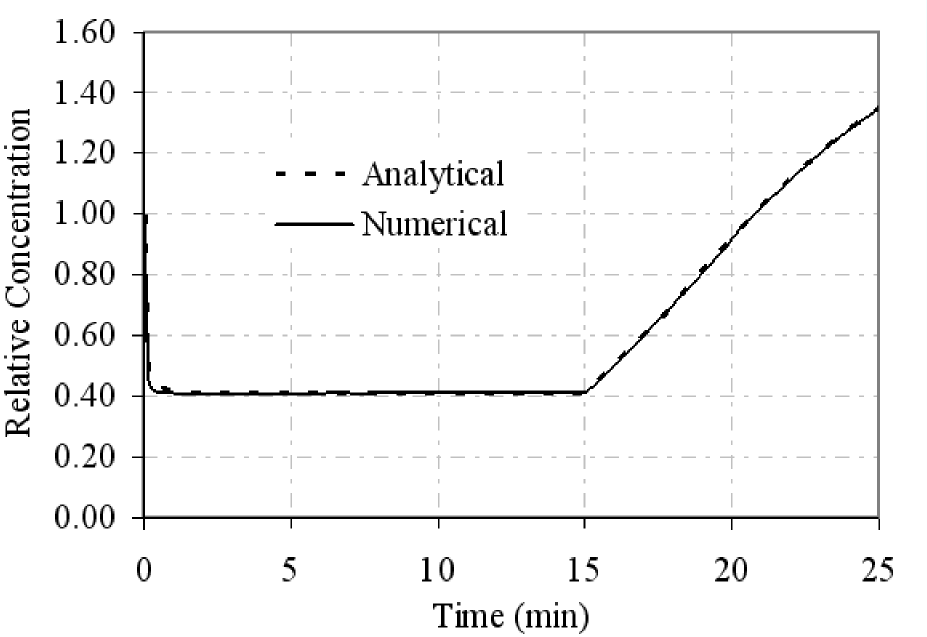

Modeling Pollutant Release from a Surface Source during Rainfall-Runoff

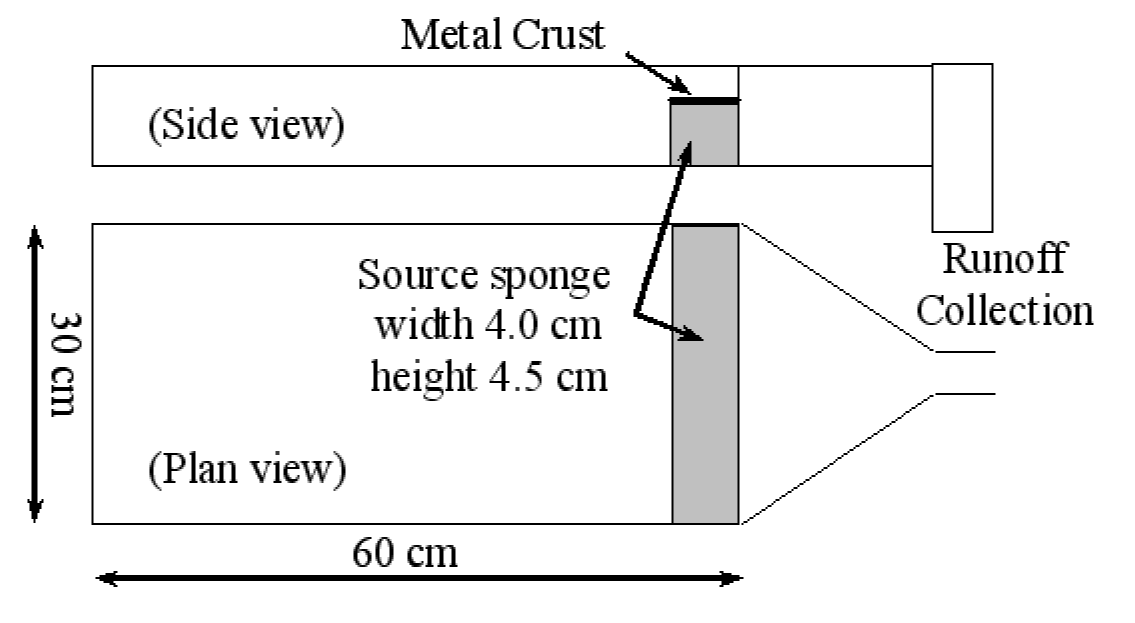

Parameters:

Slope: 0.065

Manning's n: 0.05

Intensity: 24 mm/hr

Duration: 30 min

Diffusivity: 2×10-5 cm^2/s

(Walter et al., 2001)

1. Complete or full crusting (a metal cover over the entire source)
2. No crust on the source (no metal cover over the source)
3. 50% crusting (a metal cover over half the source's top surface)

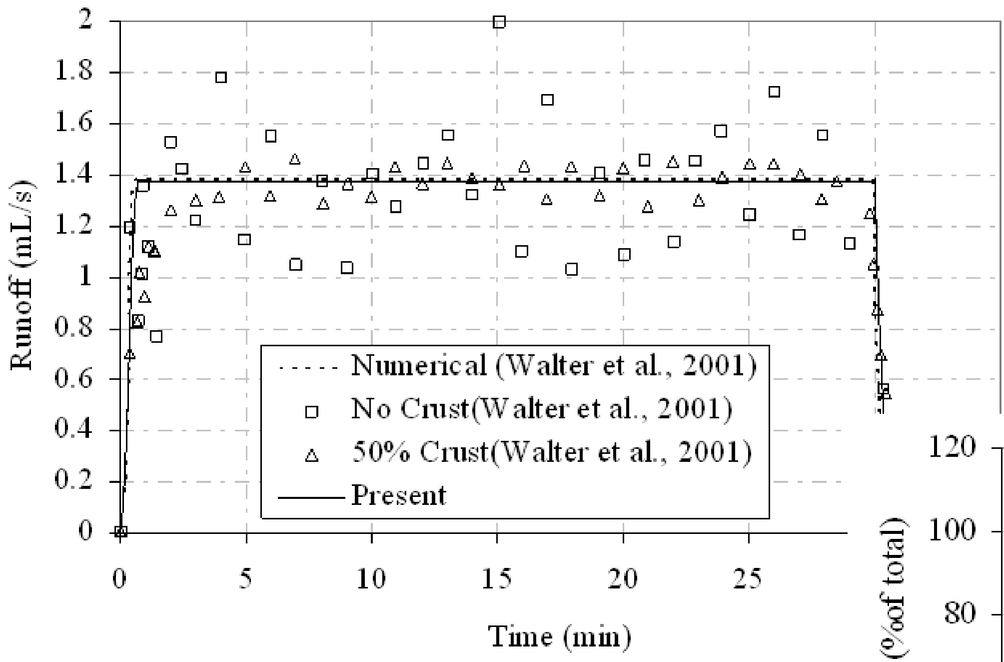

Runoff (mL/s)
Time (min)
Numerical (Walter et al., 2001)
No Crust(Walter et al., 2001)
50% Crust(Walter et al., 2001)
Present

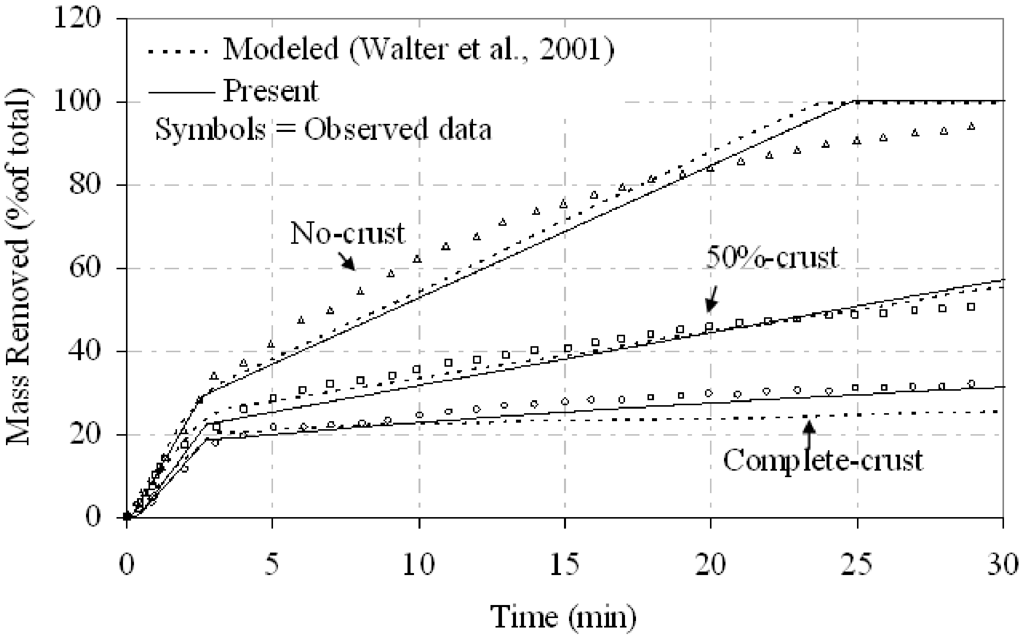

Mass Removed (%of total)
Time (min)
Modeled (Walter et al., 2001)
Present
Symbols = Observed data
No-crust
50%-crust
Complete-crust

Simulation of Coupled Surface-Subsurface Flow and Contaminant Transport

Parameters:

Box: 140 × 8 × 120 cm

Slope: 12^o

Porosity of sand: 0.34

Roughness: 0.05 s/$cm^{1/3}$

Rainfall: 4.3 cm/hr

Diffusivity: 1.2×10^{-5} cm^2/s

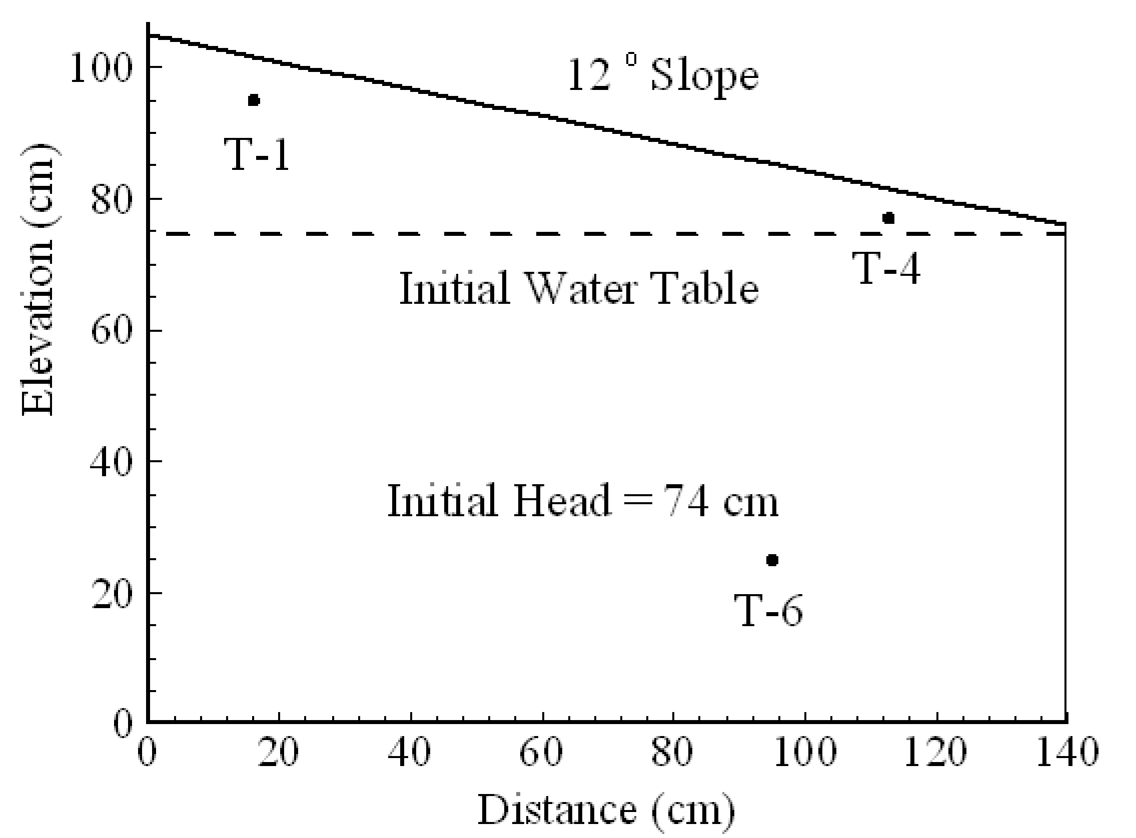

Tracer concentration: 60.6 mg/l

Hydraulic conductivity: 3.5×10^{-3} cm/s

Saturated water content: 0.335

Residual water content: 0.15

(*Abdul, 1985*)

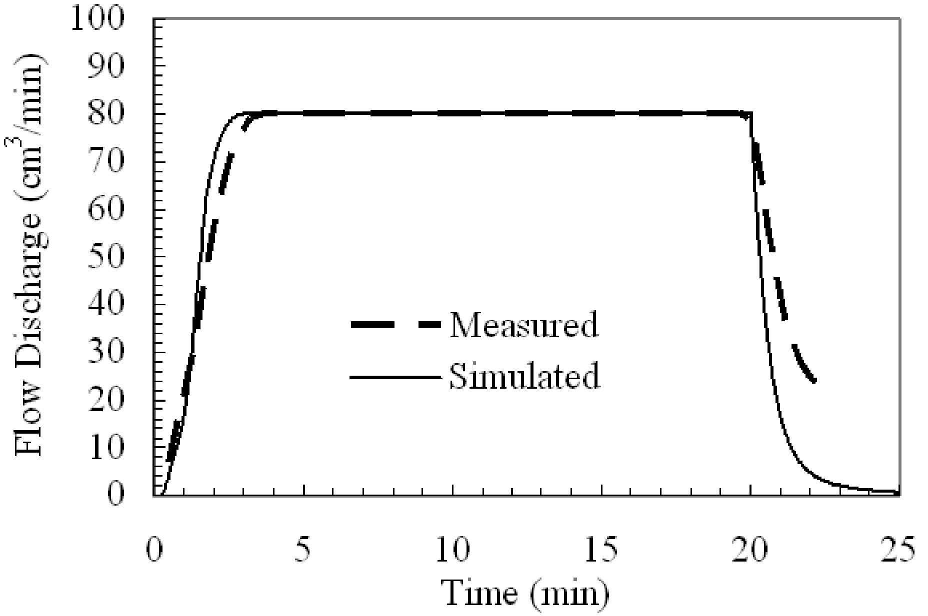
Flow Discharge (cm^3/min)
100
90
80
70
60
50
40
30
20
10
0
0
5
10
15
20
25
Time (min)
Measured
Simulated

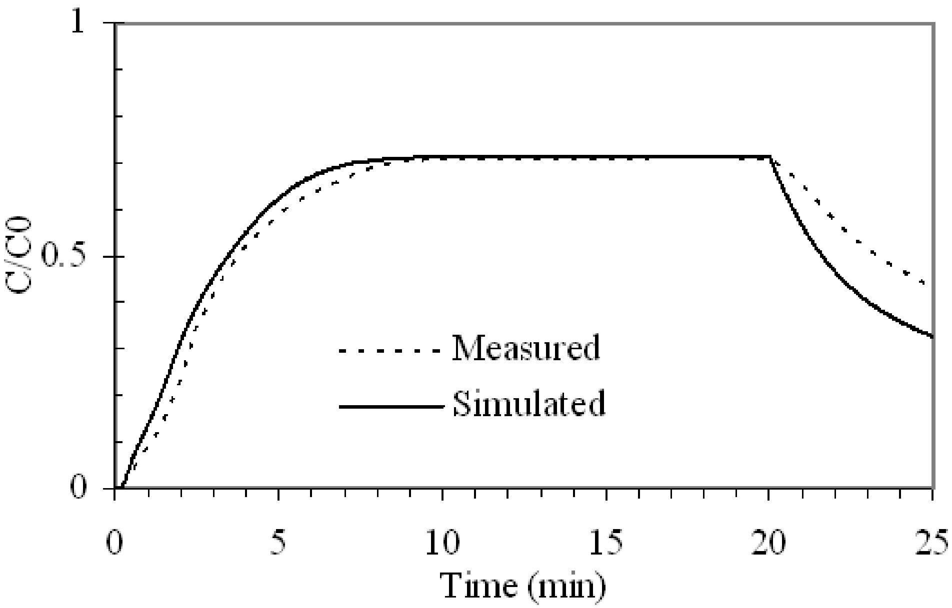
C/C0
1
0.5
0
0
5
10
15
20
25
Time (min)
Measured
Simulated

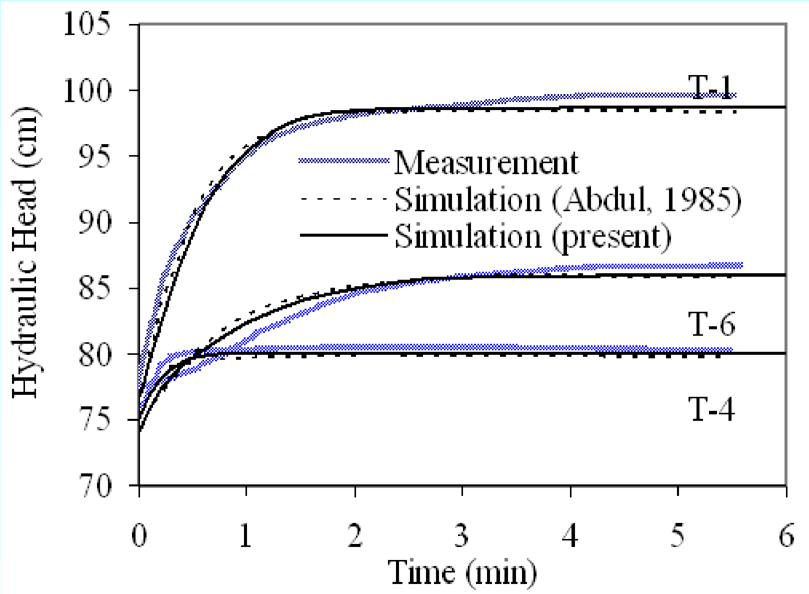
Hydraulic Head (cm)
105
100
95
90
85
80
75
70
0
1
2
3
4
5
6
Time (min)
T-1
T-6
T-4
Measurement
Simulation (Abdul, 1985)
Simulation (present)

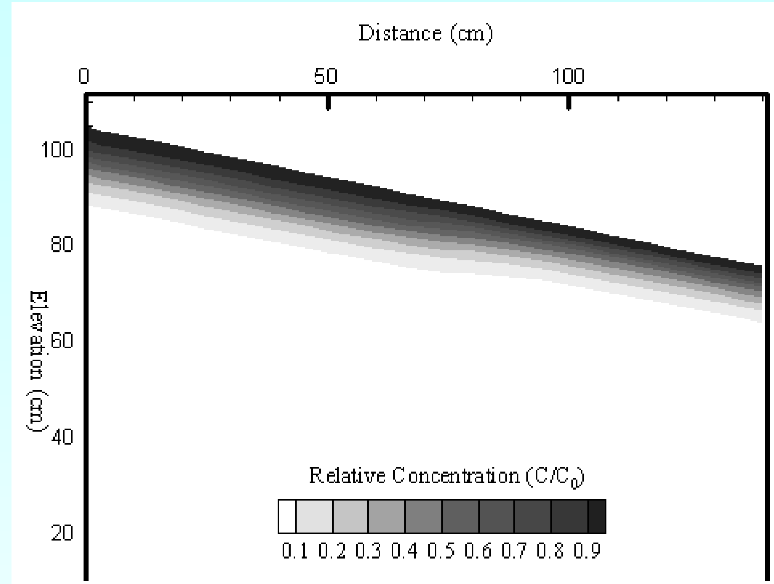
Distance (cm)
0
50
100
Elevation (cm)
100
80
60
40
20
Relative Concentration (C/C0)
0.1 0.2 0.3 0.4 0.5 0.6 0.7 0.8 0.9

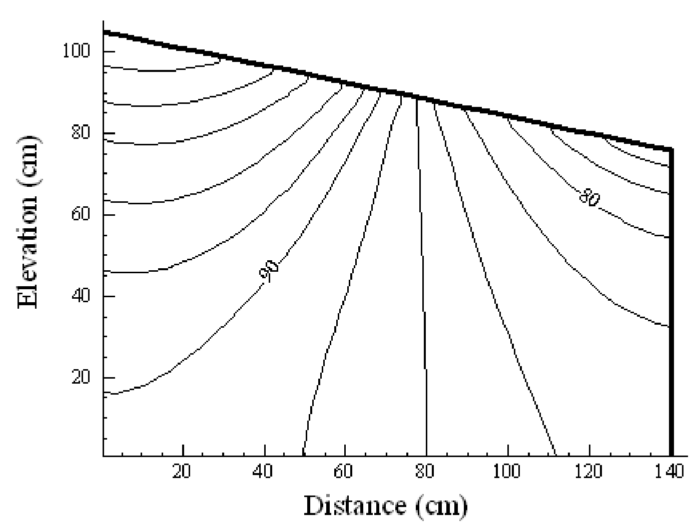
Elevation (cm)
100
80
60
40
20
90
80
20
40
60
80
100
120
140
Distance (cm)

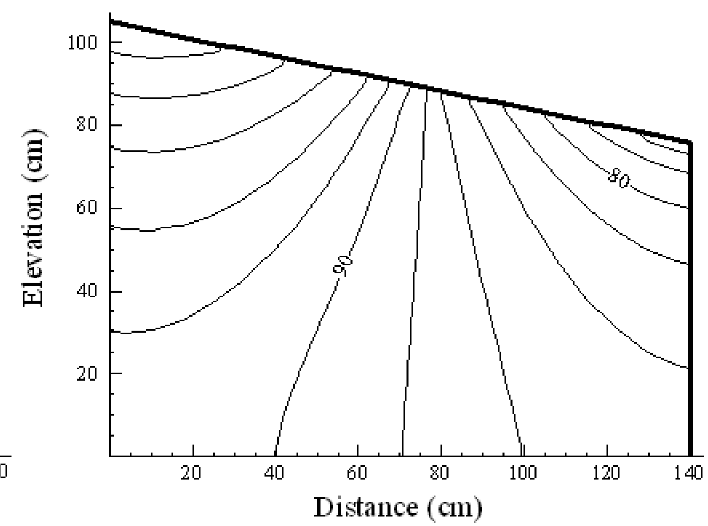
Elevation (cm)
100
80
60
40
20
90
80
20
40
60
80
100
120
140
Distance (cm)

Application – Deep Hollow Lake Watershed

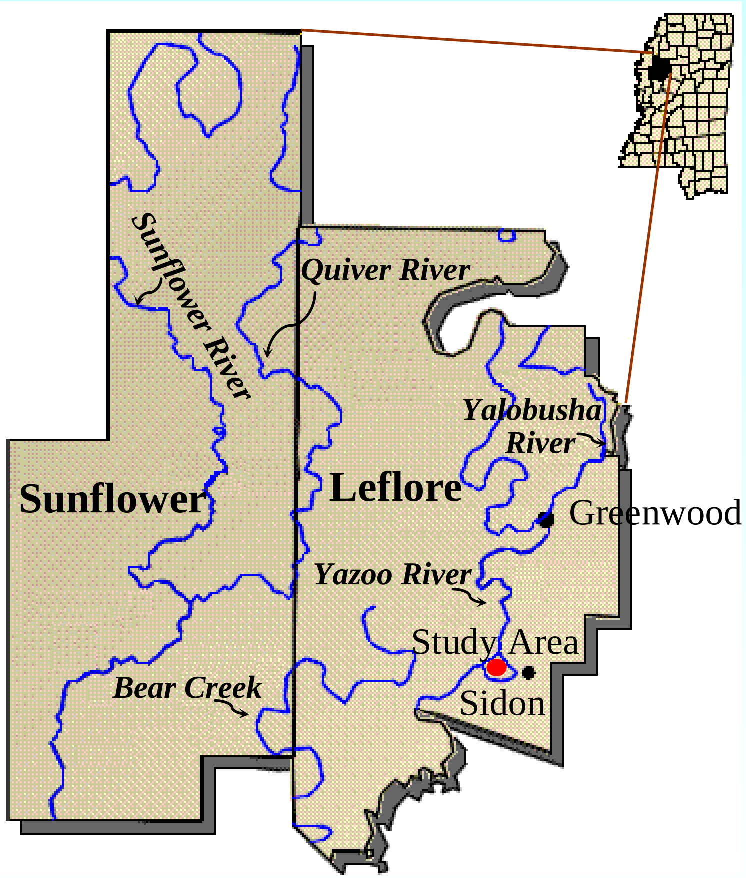

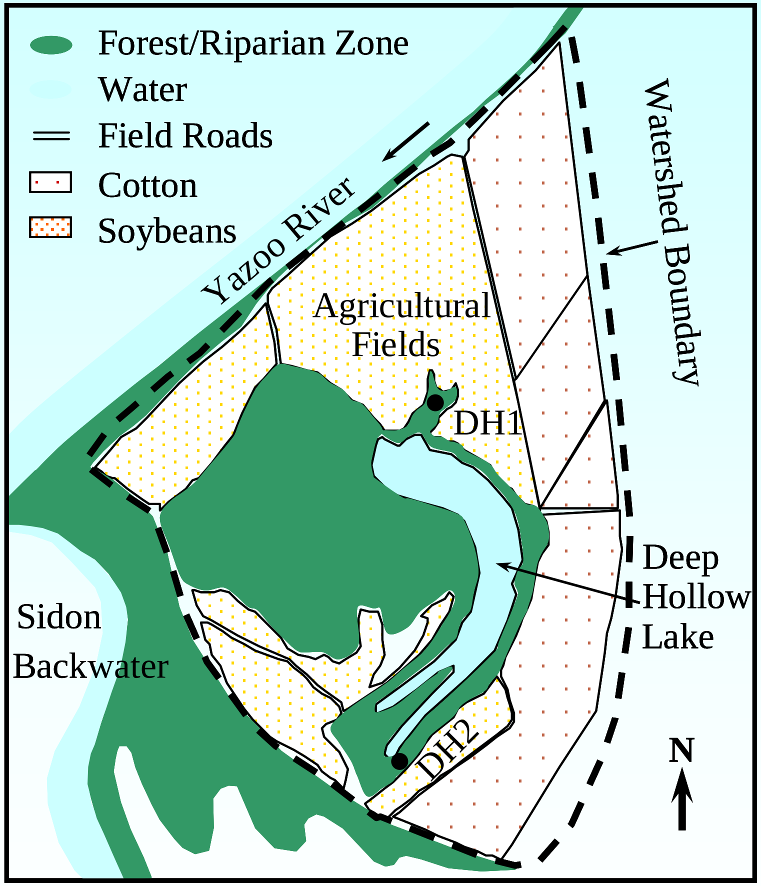

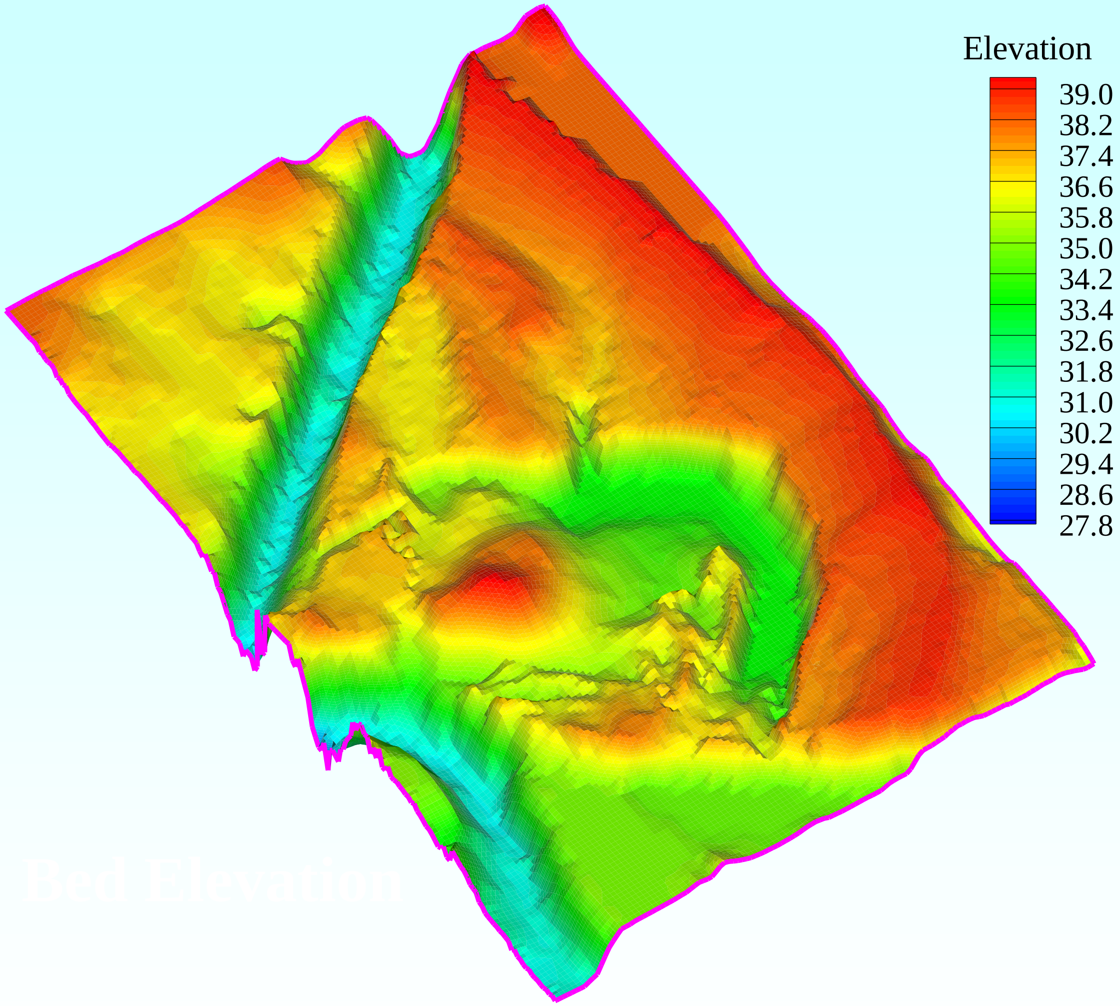

Simulation

Storm event:

February 10, 1998

February 15, 1998

Soil type:

6 types of soil, Yuan and Bingner, (2002)

Clay, silt and sand

Hydraulic conductivity of soils varies from 8.33×10^{-8} - 7.72×10^{-6} m/s.

The percentage of clay in soils from the farms varies from 20% to 50%.

Mean grain diameter (d_{50}) within the watershed ranged from 0.002 to 0.090 mm.

Field Symbol	Alpha Symbol	Map Unit
12A	AgA	Alligator clay, 0-1 percent slopes (rarely flooded)
12B	AgB	Alligator clay, 1-3 percent slopes (rarely flooded
178B	AsB	Askew silt loam, 1-3 percent slopes, (rarely flooded)
102	An	Arents, loamy
164B	DuB	Dubbs very fine sandy loam, 1-3 percent slopes
178A	DnA	Dundee loam, 0-1 percent slopes, rarely flooded
190A	Fao	Falaya silt, 0-2 percent slopes, occasionally flooded
194	AF	Arkabulla and Falaya soils, frequently flooded
284B	TnB	Tensas silty clay loam, 1-3 percent slopes (rarely flooded)
284C	TnC	Tensas silty clay loam, 3-7 percent slopes (rarely flooded)
290	TA	Tensas-Alligator complex, 0-3 percent slopes, occasionally flooded

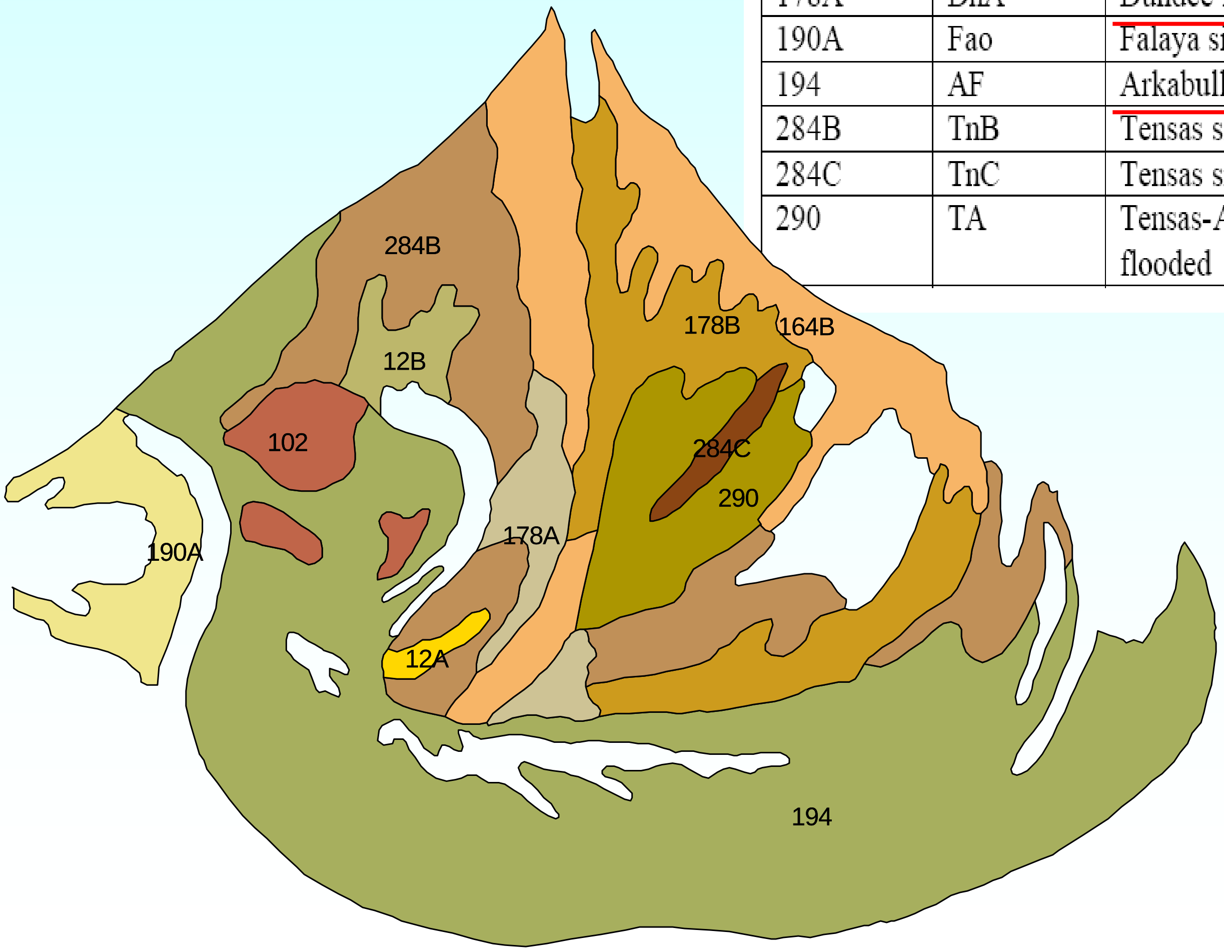

A large percentage of the sediment fell within 0.063-0.250 mm (sand) as well as within the <63 mm (silt). (Adams, 2001)

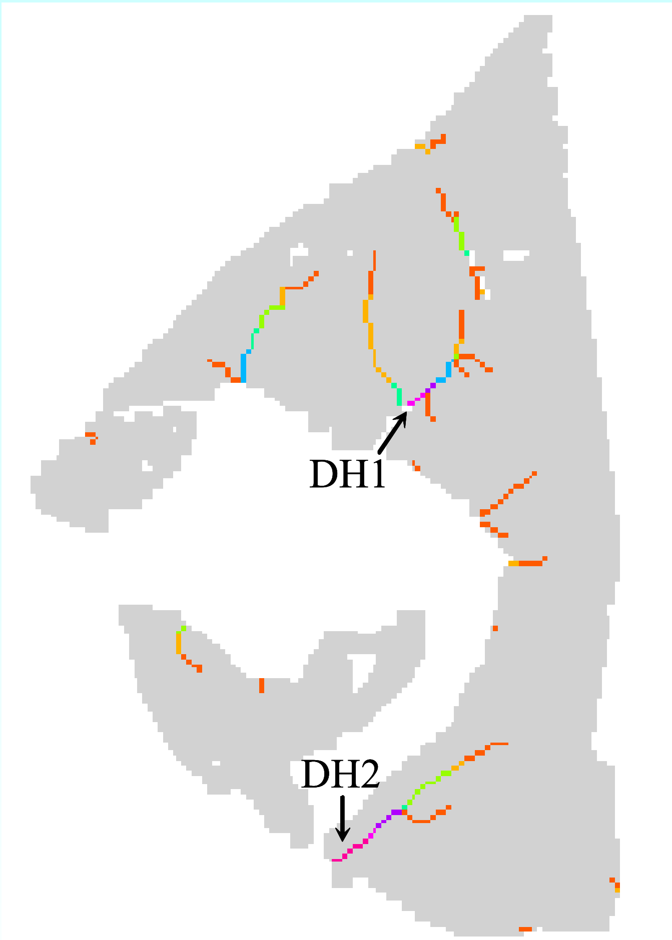

Location of main channels generated by ArcGIS

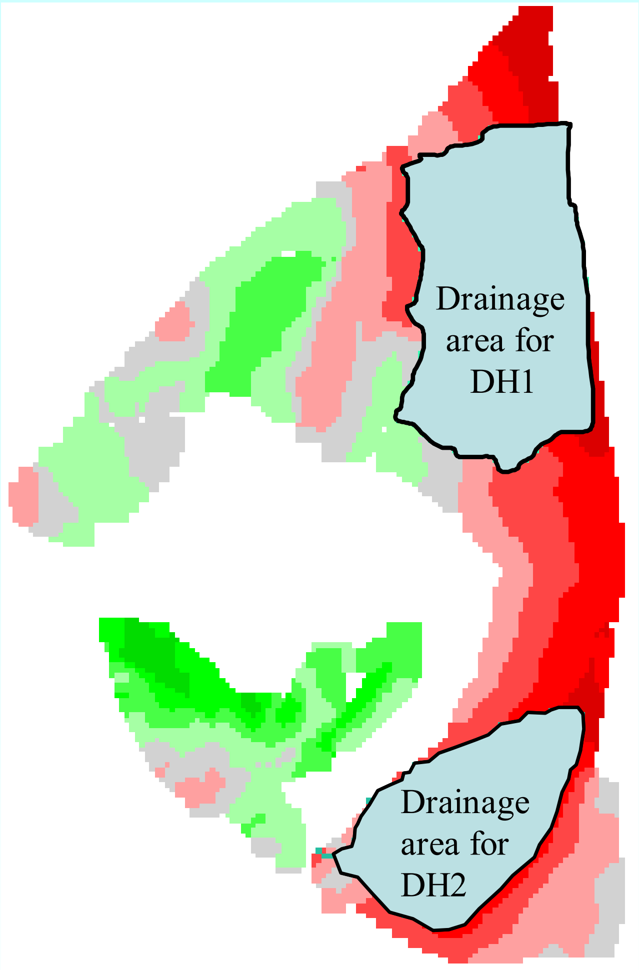

Drainage areas for two main channels generated by ArcGIS

Properties of several soils within the Deep Hollow Lake watershed

Name		Alligator silty clay	Dundee loam	Forestdale silty clay	Dowling clay	Sharkey
Hydraulic conductivity (m/s)		1.26×10^{-6}	5.96×10^{-6}	9.17×10^{-7}	3.15×10^{-7}	8.1×10^{-7}
Bulk density (g/cm^3)		1.4	1.5	1.5	1.4	1.4
Saturated water content (-)		0.378	0.266	0.292	0.416	0.412
Residual saturation (-)		0.156	0.048	0.083	0.197	0.197
Field capacity suction (m)		4.01	3.26	4.13	3.4	3.4
van Genuchten parameters	a	0.01	0.01	0.01	0.01	0.01
	m_1	0.22	0.25	0.27	0.21	0.21
	m_2	1.28	1.34	1.36	1.27	1.27

Land use parameter values for the calibration run

Land cover	Forest	Cotton	Soybean	Pasture	Water
Roughness	0.1	0.05	0.04	0.08	0.01

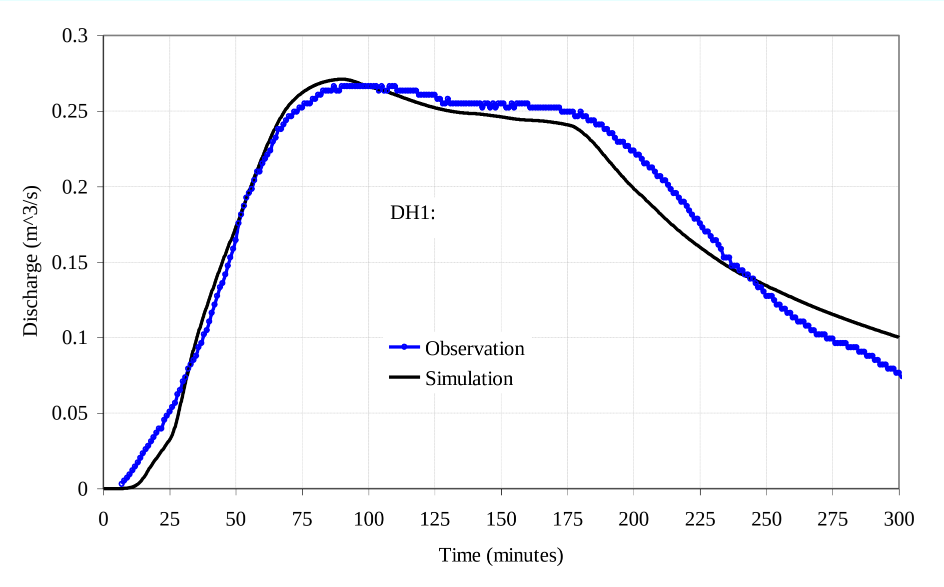

This event began at 19:00 pm

Duration:	**4.5 hr**
Total rainfall depth:	**22.6±2.0 mm**
Average rainfall rate:	**5.0 mm/hr**
Maximum rate:	**28.4 mm/hr**

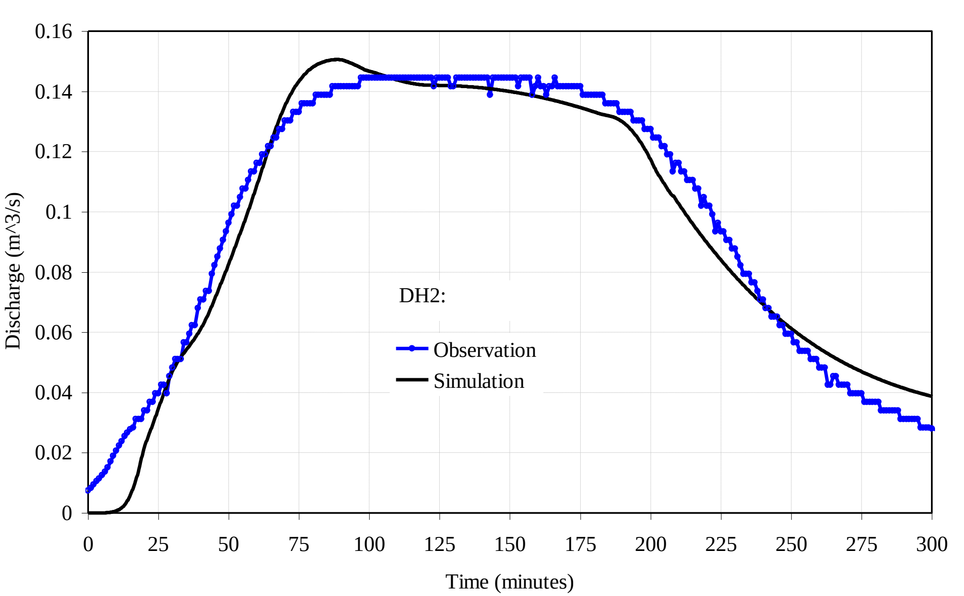

Initial water elevation in the river: 34.14 m
Initial water elevation in the lake: 35.04 m

Hydrographs at stations DH1 and DH2 on 02/10/98

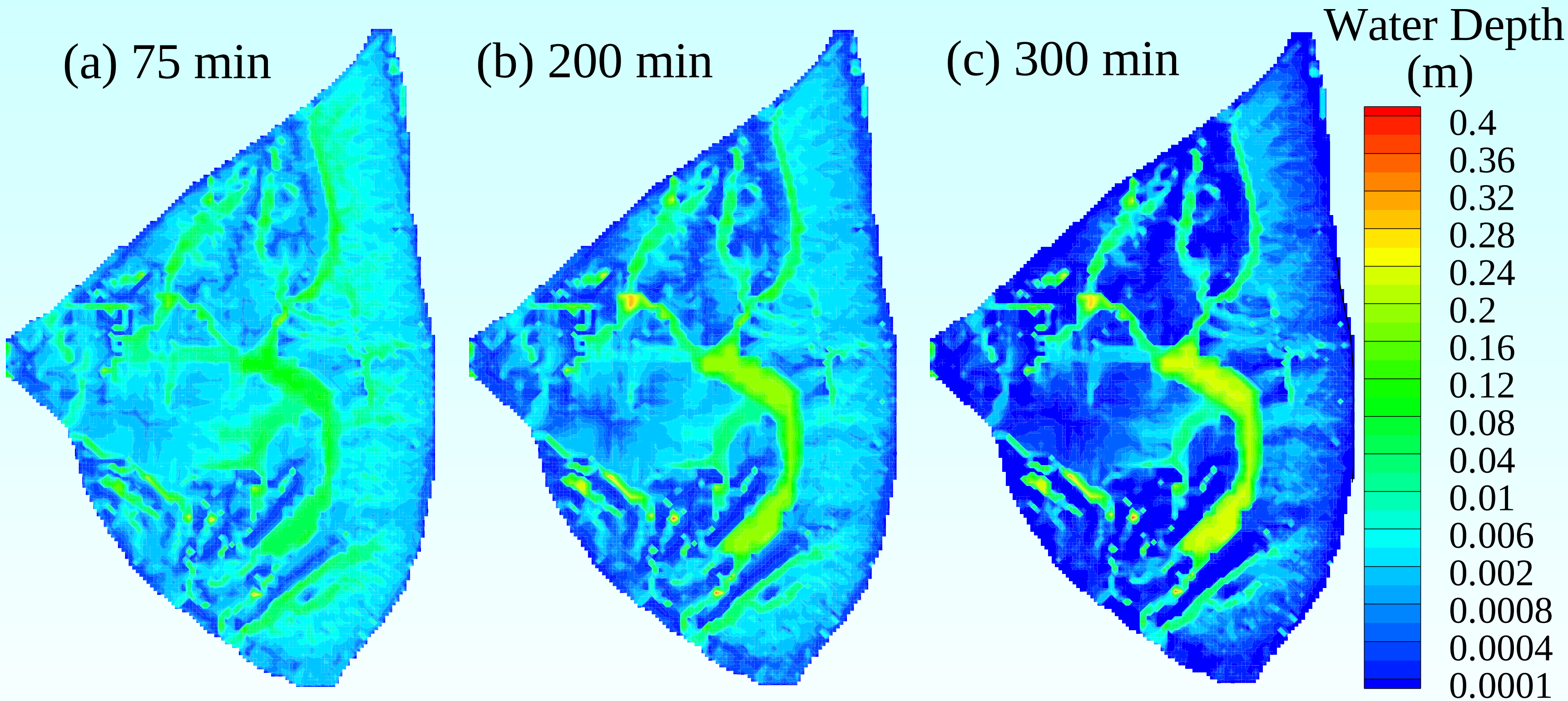

Water depth during the rainfall event on 02/10/98

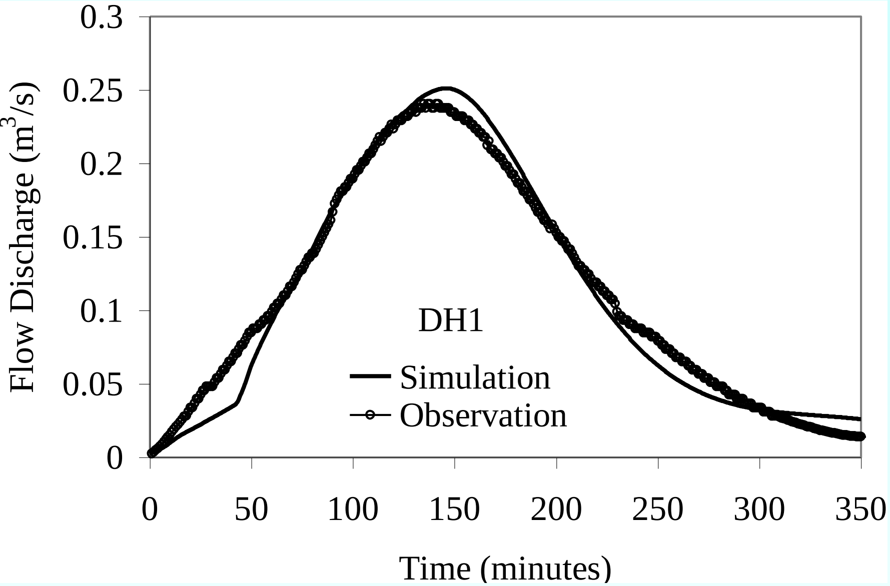

The rainfall event had a little rainfall.
Averaged rainfall intensity: 1.5 mm/hr
Maximum rate: 3.0 mm/hr
Total rainfall depth: 9.0±2.0 mm

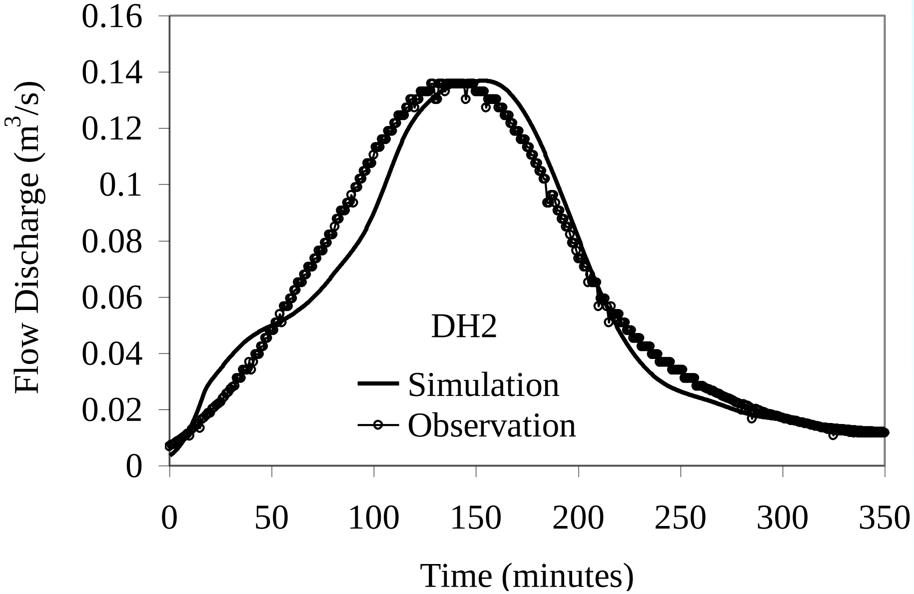

Simulation time: 6 hours
Wet condition

Hydrographs at stations DH1 and DH2 on 02/15/98

The sediment size in the simulation is classified as clay, silt, and sand.

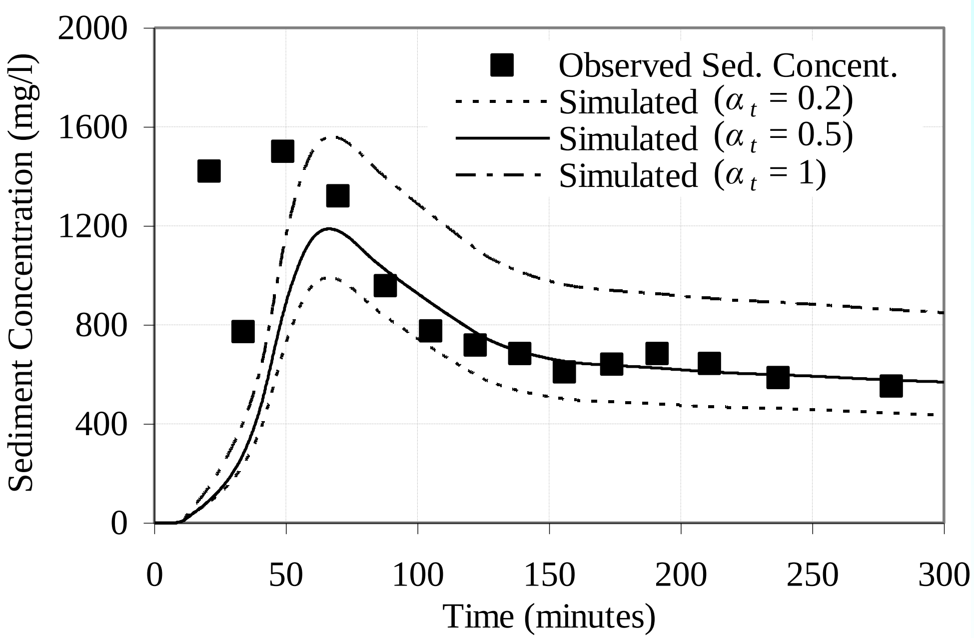

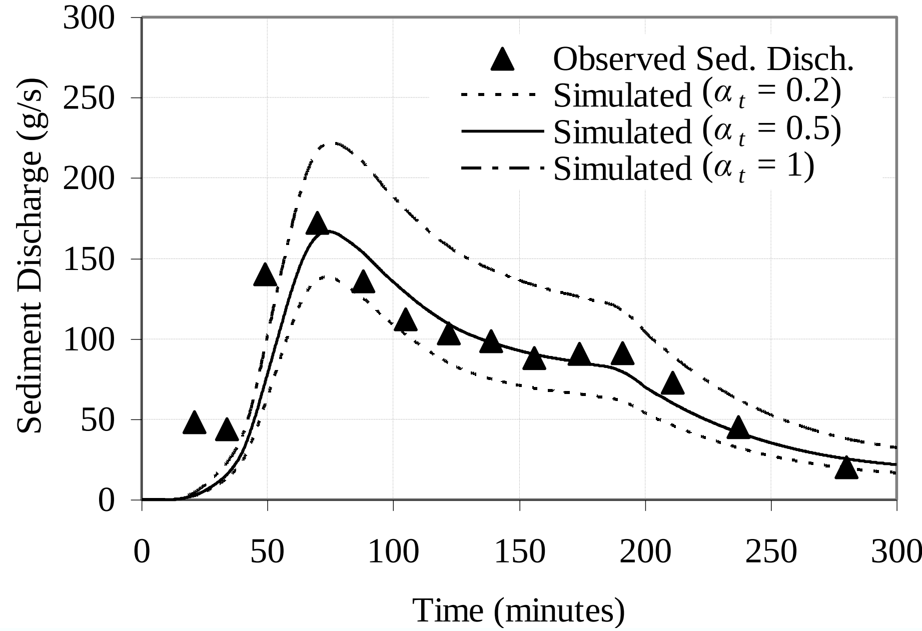

Sediment concentration and discharge at station DH2 on 02/10/98

using difference coefficient α_t

Conditions:

- **The storm event on May 29 began around 1:15 am and lasted for about 8.5 hr.**
- **The total rainfall depth for this storm event: 86 mm**
- **The average rainfall intensity: 10 mm/hr**
- **Maximum intensity: 58.9 mm/hr**
- **Simulation time of this rainfall-runoff event: 10 hr**
- **Roughness coefficients of cotton and soybean fields: 0.065 , 0.06**
- **A dry condition is used as the initial condition.**
- **Water elevation in the river: 32.6 m**
- **Water elevation in the lake: 34.6 m**
- **The diffusivity for Fluometuron used in the simulation: 1.67×10^{-5} cm^2/s**
- **The sediment size in the simulation: clay, silt, sand**

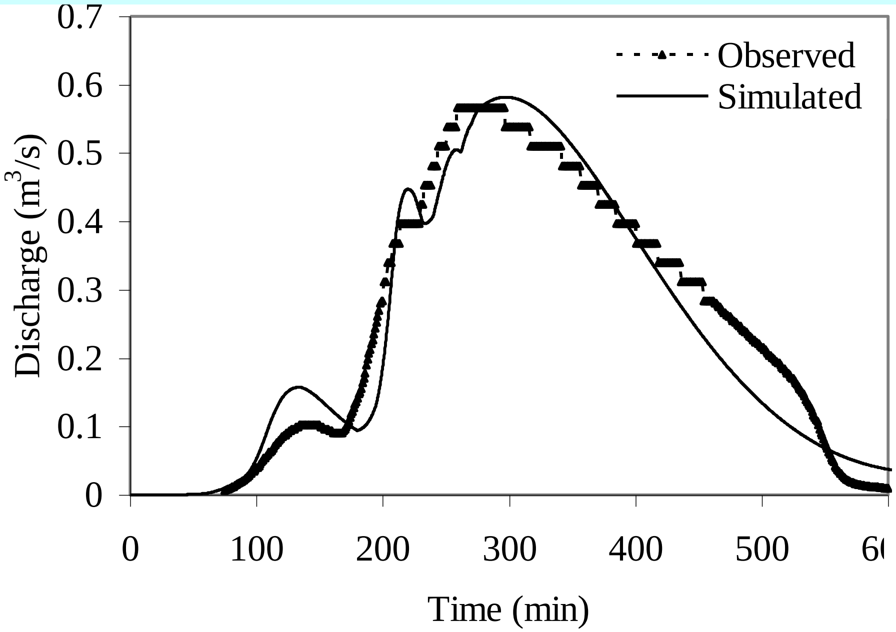

Flow discharges at DH2 on 5/29/98

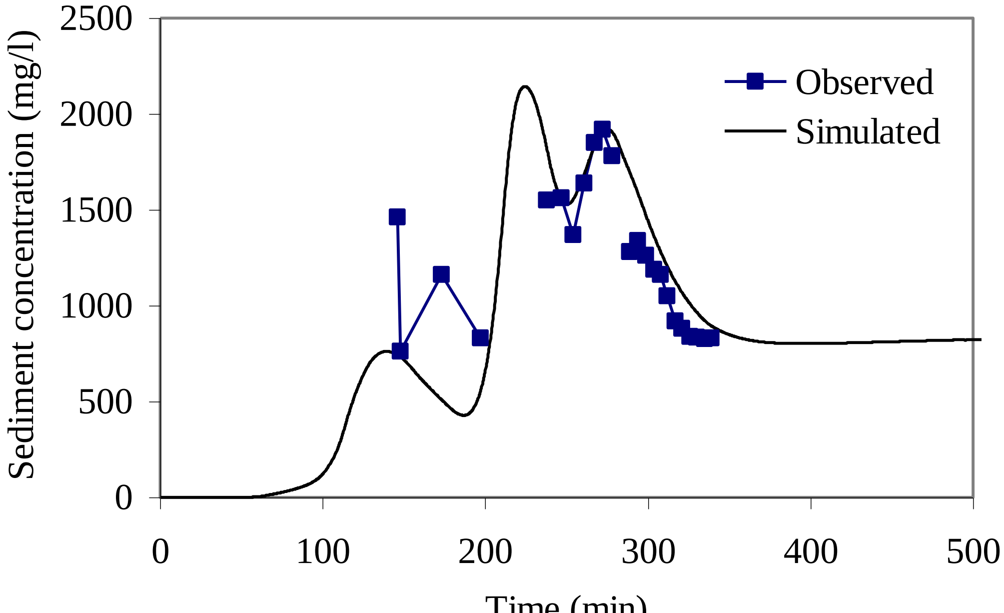

Sediment concentrations at DH2 on 5/29/98

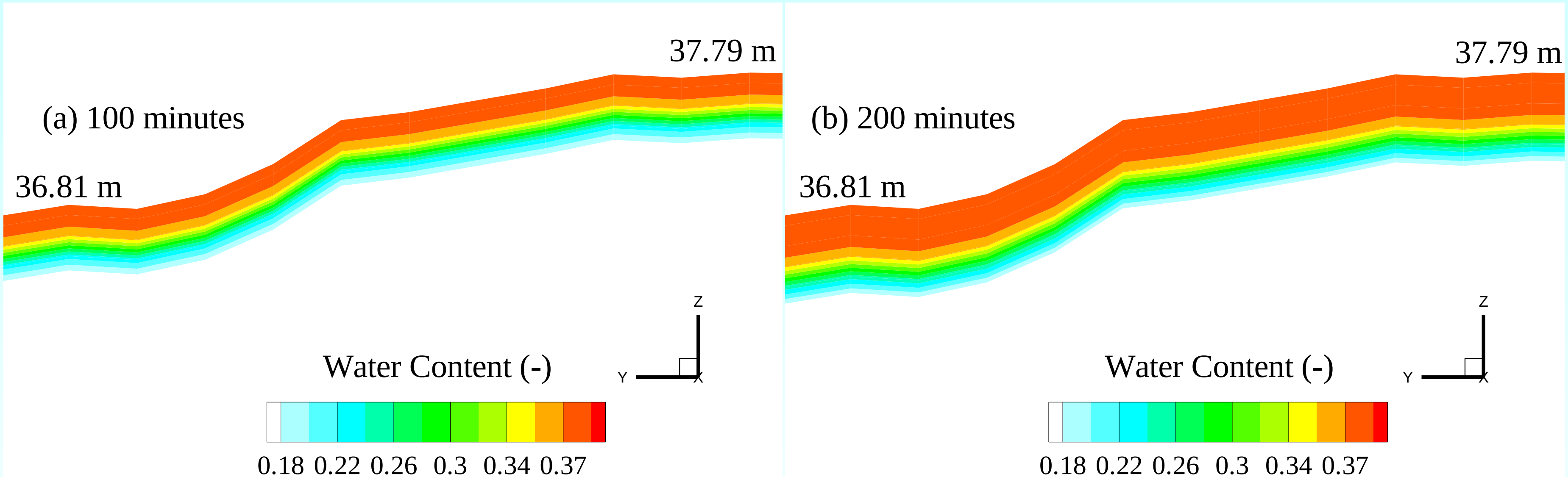

Distribution of water content at the section of *x* = 756855 m at different times

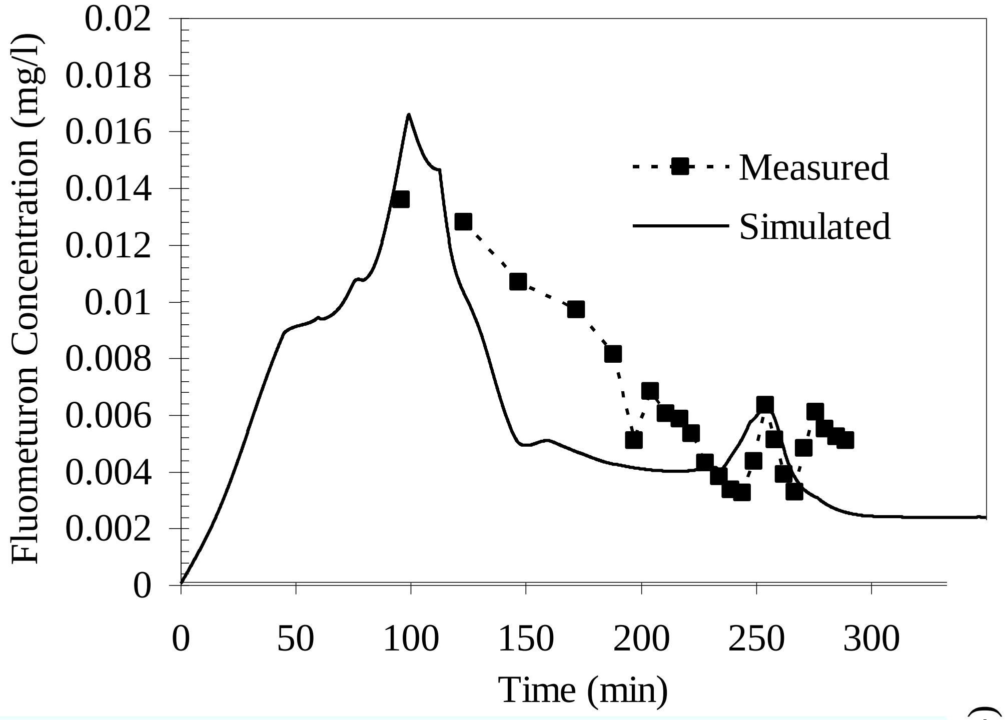

Measured and simulated Fluometuron concentrations at DH2 on 5/29/98

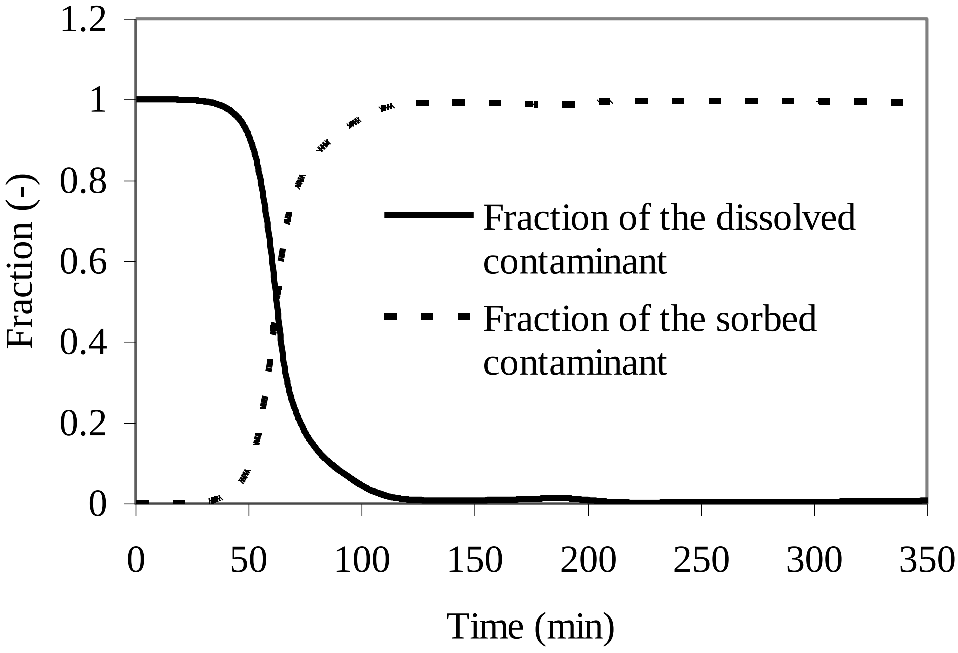

Fractions of the dissolved and sorbed contaminants

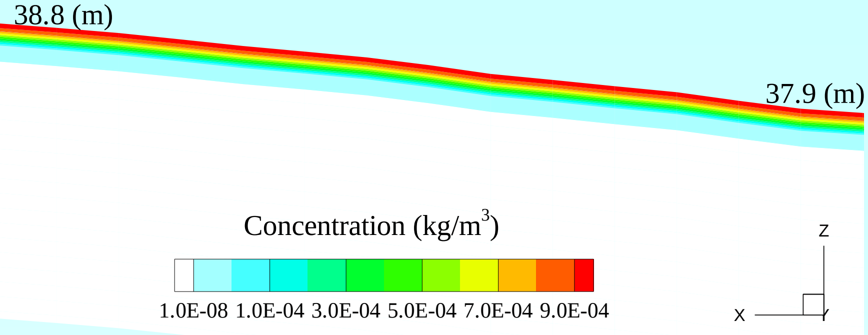

Concentration of Fluometuron in the subsurface domain at the section of *y* = 3700525 m at 200 minutes

Sensitivity of Fluometuron concentration to dissolution rate coefficient and mass exchange coefficient

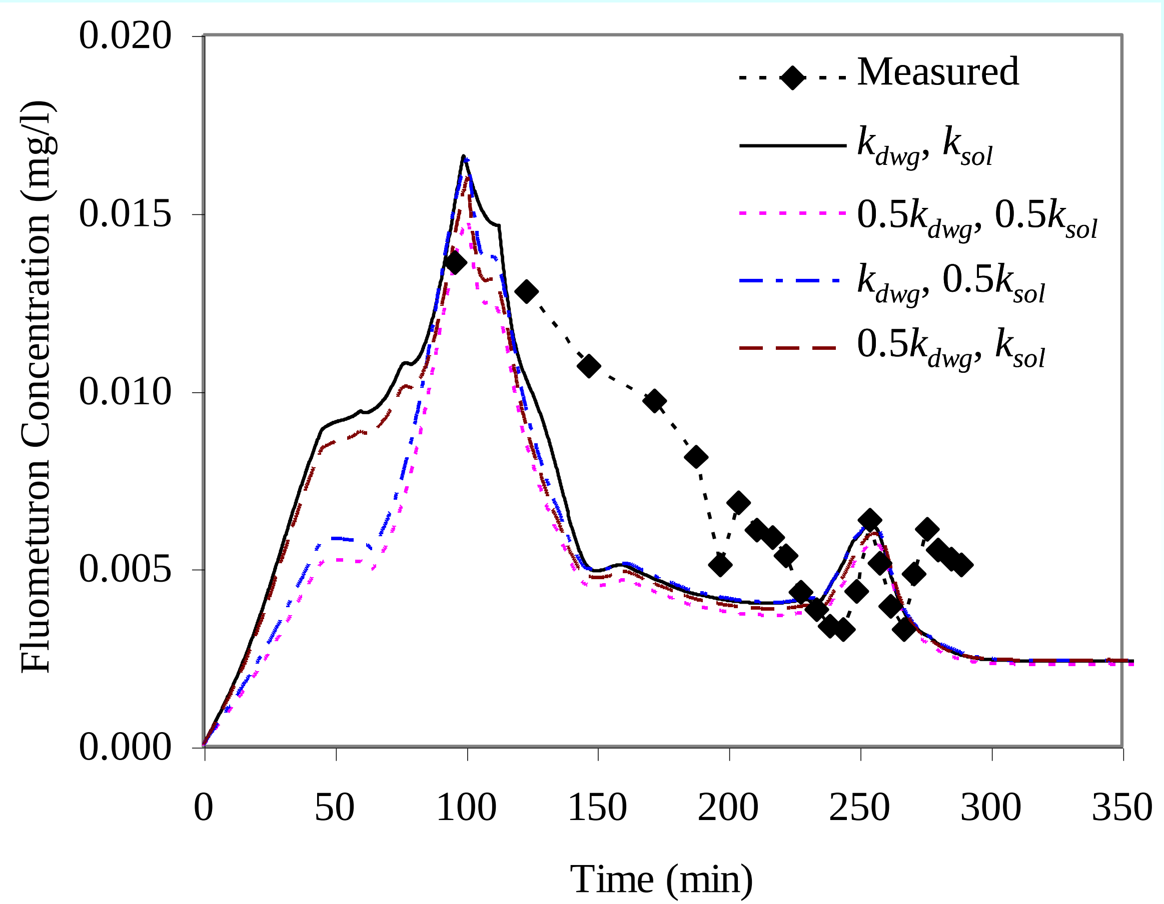

Summary and Conclusions

1. This dissertation research has established a physically-based integrated numerical model for flow, sediment and contaminant transport in the surface-subsurface system at the full catchment scale.

2. A general framework for coupling the surface and subsurface flow equations is developed, rather than the traditional conductance concept.

3. Sediment transport due to overland flow is modeled using the nonequilibrium concept that considers both erosion and deposition. The model simulates nonuniform total-load sediment transport, taking into account detachment by rainsplash and hydraulic erosion by surface flow.

4. Contaminant transport model in the integrated surface/subsurface system is described using the advection-diffusion equation, which considers the exchange between surface and subsurface as well as the effect of sediment sorption and desorption.

Summary and Conclusions

5. The integrated surface-subsurface flow, sediment, and contaminant transport model has been tested and verified by comparing numerical solutions with several sets of analytical solutions, experimental data, and field data. It has been further applied to compute flow discharge, suspended sediment, and herbicide concentration during storm events in the Deep Hollow Lake watershed, Mississippi.

6. The simulation shows that the influence of sediment sorption and desorption on the contaminant concentration is important when the rainfall-runoff related upland soil erosion and transport exist. The sensitivity of the model to several parameters is also evaluated.

7. The results have shown that the integrated model framework is capable of simulating the flow, sediment, and contaminant transport processes in natural surface-subsurface systems.

Publications Related

Z. He (2007). “Numerical simulation of flow, sediment, and contaminant transport in integrated surface-subsurface systems.” PhD Dissertation, The University of Mississippi, USA.

Z. He, W. Wu, and S. S.Y. Wang (2008). “Coupled finite-volume model for 2-D surface and 3-D subsurface flows,” J. Hydrologic Eng., ASCE, 13(9), 835–845.

Z. He, W. Wu, and S. S.Y. Wang (2009). “An integrated two-dimensional surface and three-dimensional subsurface contaminant transport model considering soil erosion and sorption,” J. Hydraulic Eng., ASCE, 135(12), 1028–1040.

Z. He and W. Wu (2009). “A physically-based integrated numerical model for flow, upland erosion, and contaminant transport in surface-subsurface systems,” Science in China, Series E - Technological Sciences, 52(11), 3391–3400, doi: 10.1007/s11431-009-0335-6.